Applied Energy 353 (2024) 122132

Contents lists available at ScienceDirect

Applied Energy

journal homepage: www.elsevier.com/locate/apenergy

Costs, carbon footprint, and environmental impacts of lithium-ion batteries – From cathode active material synthesis to cell manufacturing and recycling

Moritz Gutsch [a,b,*], Jens Leker [a,b]

[a] Helmholtz Institute Münster, IEK-12, Forschungszentrum Jülich GmbH, Corrensstraße 46, Münster 48149, Germany
[b] Institute of Business Administration at the Department of Chemistry and Pharmacy, University of Münster, Leonardo Campus 1, Münster 48149, Germany

HIGHLIGHTS

- CAM synthesis accounts for >45% of costs, CO2eq and combined environmental impacts.
- Recycling costs of < $9 kWh-1 are small compared to manufacturing costs of $95 kWh^{-1}.
- Recycling reduces normalized & weighted environmental impact of cells by 75%.
- Benefit of recycling on CO2eq emissions is comparably small.
- Low scrap improves costs and environmental impacts more than low-carbon energy.

GRAPHICAL ABSTRACT

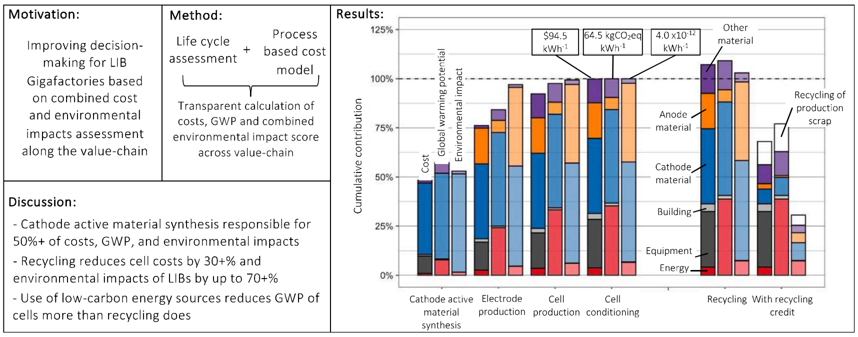

Motivation:

Improving decision-making for LIB Gigafactories based on combined cost and environmental impacts assessment along the value-chain

Method:

Life cycle assessment + Process based cost model

Transparent calculation of costs, GWP and combined environmental impact score across value-chain

Discussion:

- Cathode active material synthesis responsible for 50%+ of costs, GWP, and environmental impacts
- Recycling reduces cell costs by 30+% and environmental impacts of LIBs by up to 70+%
- Use of low-carbon energy sources reduces GWP of cells more than recycling does

Results:

ARTICLE INFO

Keywords:
Battery cost
Battery carbon footprint
Battery environmental impact
Battery recycling
Battery manufacturing
Life cycle assessment

ABSTRACT

Strong growth in lithium-ion battery (LIB) demand requires a robust understanding of both costs and environmental impacts across the value-chain. Recent announcements of LIB manufacturers to venture into cathode active material (CAM) synthesis and recycling expands the process segments under their influence. However, little research has yet provided combined costs and environmental impact assessments across several segments of the LIB value-chain. To address this gap, we provide a combined cost assessment and life cycle assessment (LCA), covering CAM synthesis, cell manufacturing and hydrometallurgy recycling. 1 kWh cell capacity (NMC_{811}-C) is chosen as functional unit. Results for cell manufacturing in the United States show total cell costs of $94.5 kWh^{-1}, a global warming potential (GWP) of 64.5 $kgCO_2eq$ kWh^{-1}, and combined environmental impacts (normalizing and weighing 16 impact categories) of 4.0×10^{-12} kWh^{-1}. Material use contributes 69% to costs and 93% to combined environmental impacts. Energy demand, meanwhile, accounts for 35% of GWP. Initially, hydrometallurgy recycling adds 5 to 10% to total costs, GWP, and environmental impacts. Including recycling credits, as recycled material substitutes new virgin material, shows benefits for recycling. Combined environmental impacts benefit most from recycling (−75%), followed by costs (−44%) and GWP (−37%). Further, we present a comprehensive dashboard which reveals how different scenarios, such as, using wind power instead of grid electricity, influence costs, GWP, and environmental impacts across process segments. Switching to low-carbon energy, for example, reduces GWP more than recycling would. Also, our dashboard shows that

---

* Corresponding author at: Helmholtz Institute Münster, IEK-12, Forschungszentrum Jülich GmbH, Corrensstraße 46, Münster 48149, Germany.
E-mail address: m.gutsch@fz-juelich.de (M. Gutsch).

https://doi.org/10.1016/j.apenergy.2023.122132
Received 28 June 2023; Received in revised form 14 September 2023; Accepted 13 October 2023

recycling or low scrap are more suitable options if reduction of costs or combined environmental impacts is the objective.

1. Introduction

Demand for high capacity lithium-ion batteries (LIBs), used in stationary storage systems as part of energy systems [1,2] and battery electric vehicles (BEVs), reached 340 GWh in 2021 [3]. Estimates see annual LIB demand grow to between 1200 and 3500 GWh by 2030 [3,4]. To meet a growing demand, companies have outlined plans to ramp up global battery production capacity [5]. The production of LIBs requires critical raw materials, such as lithium, nickel, cobalt, and graphite. Raw material demand will put strain on natural resources and will increase environmental problems associated with mining [6,7]. As ore grades for key battery metals such as copper and nickel decrease, high efficiency in upstream and downstream operation alongside low-carbon energy sources is essential to limit its environmental impact [8]. Next to environmental issues of raw material extraction, supply chain bottlenecks present challenges for manufacturers [9,10]. Access to batteries has become a top priority for automotive companies [10].

Economies of scale will continue to decrease the share of processing costs on total LIB costs [11,12]. The relative share of material cost is set to increase. Consequently, volatility in raw material prices present risks to cost competitiveness. Developing new mining projects alongside a sustained effort to establish a well-functioning collection and recycling system for LIBs is needed to reduce long-term needs for raw material extraction. Integration of recycling into the framework of Gigafactories, which produce LIBs with an annual capacity of more than one GWh, is promising. For example, Northvolt, a Swedish battery company, works on integrating a LIB recycling factory into its Gigafactory layout [13].

An integrated understanding of costs and environmental impacts along the value chain of battery production and recycling is central to strategic decision-making [14]. Regulations, such as in the European Union (EU), will make the carbon footprint of LIBs subject to upper limits as soon as 2027 [15]. The EU legislation, for now, is most concerned with CO_2 emissions, commonly expressed through global warming potential (GWP) in kg CO_2 equivalents [15]. However, conducting life cycle assessments (LCAs) with several environmental impact categories presents additional insight [16].

Reviewing academic literature we find that most publications look either at economic or environmental aspects of lithium-ion batteries (see supplementary material, Tables A1-A3). Of the few studies that cover both economic and environmental aspects [17–19], CO_2 emissions have been of most prominence. Combined cost and environmental impact assessments, consequently, are largely missing in literature, despite growing interest from the industry experts [14,20]. Furthermore, limited work has covered both production and recycling of cells within a shared technical framework, which is another research gap.

Addressing these challenges, the present work contributes an integrated process-based cost model and life cycle assessment for industrial-scale cathode active material (CAM) synthesis, cell manufacturing, and hydrometallurgy recycling. Using a shared functional unit of 1 kWh cell capacity, and the same cell and process layouts for both cost and environmental assessments provides a high level of transparency. Our environmental impact assessment includes but is not limited to global warming potential as is recommended by experts [21,22]. Further, we conceive a novel, original dashboard that comprehensively presents costs, CO_2 emissions and combined environmental impacts –split into contributions of cathode material, anode material, other material, energy, equipment, and building– for each process. This dashboard allows to evaluate the influence of changes in process design or parameters on economic and environmental results, while at the same time indicating in which part of the process most changes occur. This will support strategic decision-making of stakeholders in the battery industry.

Due to its high popularity in automotive applications [3,23], outstanding specific energy [24], as well as competitive cost [11] and carbon footprint [25], we select a state-of-the-art lithium nickel manganese cobalt oxide battery (NMC_{811}), as currently manufactured by, for example, Northvolt [26], for the present analysis. We set the United States as baseline geography for our analysis, and conduct sensitivity analyses for key parameters to broaden the applicability of our findings. Incorporating other battery technologies, such as lithium-iron phosphate (LFP) or next generation sodium-ion technologies into the combined cost and environmental assessment framework is beyond the scope of the present analysis. Nevertheless, our approach provides a way for other researchers to fit their cell design and material into our presented method and evaluate the combined costs and environmental impacts throughout the value-chain of present and future battery storage technologies.

2. Background

2.1. Raw materials

At the start of the production process, manufacturing LIBs in not much different than, for example, the production of combustion engines or smartphones. All have in common that they require raw materials. Circular economy strategies outline that mining of new raw materials should be kept to a minimum and as much recycled material as possible fed back into the material circle [27,28]. Growing LIB demand will require extraction of new raw materials for some time before a closed material loop is within reach [6,7]. Raw material extraction has become subject to public attention due to social and ecological problems [7,29,30]. Raw materials, such as lithium, nickel and cobalt go through material refining to reach battery grade purity levels [31]. Most capacity for material refining is located in Asia, with the European Union and United States encouraging a buildup of local refining capacity [9,27].

2.2. Cathode active material synthesis

Selection of cathode active material has impact on important cell characteristics such as specific energy, cycle life, and safety [35,36]. By some estimates, NMC_{811} is expected to become the dominant cathode active material within the next years [23]. NMC and other transition metal oxides are synthesized through co-precipitation and calcination [33], see Fig. 1. For high-nickel CAMs (e.g., NMC_{811}), LiOH is used as lithium source. Low-nickel CAMs (e.g., NMC_{111}) can use slightly cheaper Li_2CO_3 [33]. Calcination is an energy intensive process, with temperatures exceeding 750 °C and process duration of several hours [37]. Some battery companies have started to internalize the CAM synthesis [26].

Costs for industrial production of NMC cathode active material in the United States via co-precipitation and calcination have been calculated as \$23 kg^{-1} (NMC_{111}) and \$21.5 kg^{-1} (NMC_{811}) by Ahmed et al. [38] Innovative flame-assisted spray pyrolysis reduces costs to \$19 kg^{-1} (NMC_{111}), driven by lower operation costs [39].

Global warming potential associated with industrial synthesis of 1 kg NMC_{111} CAM in the United States was reported as 16 $kgCO_2eq$ by the Argonne National Laboratory (ANL). 43% of GWP came from energy used during co-precipitation and calcination, 57% from used raw materials [25,40]. GWP for 1 kg NMC_{811} CAM synthesized in China has been reported as 32 $kgCO_2eq$[41]. For electricity intensive processes, such as calcination of cathode active material, the carbon emission factors of the local grid, for example, 0.45 $kgCO_2eq\ kWh^{-1}$ in U.S. and 0.67 $kgCO_2eq\ kWh^{-1}$ in China [25], have a strong impact on GWP.

2.3. Cell manufacturing

Cell manufacturing consists of electrode production, cell production and cell conditioning, see Fig. 1.

Electrode production starts with mixing of electrode materials [32,42]. A common anode active material is graphite, with a practical specific capacity of 360 mAh g^{-1} and potential of 0.1 V against Li/Li^+. Efforts are underway to increase the specific capacity by adding small amounts of silicon [36]. Anode active material is mixed with conductive carbon, binder, and additives, with water used as solvent [23,43], and coated on a thin copper foil (ca. 6–8 μm thickness) [33,36]. Lithium iron phosphate (LFP) and lithium nickel cobalt manganese oxide (NMC) are frequently used CAMs [44]. LFP has a practical specific capacity of 165–170 mAh g^{-1} and a potential of 3.45 V against Li/Li^+ (ref. [24,36]). Consequently, the specific energy of the electrode active material paring of LFP and graphite (without any inactive material) is limited to 380 Wh kg^{-1}. NMC, meanwhile, shows a specific capacity of 160–190 mAh g^{-1} at a higher voltage potential of 3.7 V against Li/Li^+ (ref. [24]). Increasing the nickel content, as done in NMC_{811} compared to NMC_{111}, corresponds with specific capacities at the upper end of this range [24,33]. A specific capacity of 450 Wh kg^{-1} presents the upper limit for an NMC/Graphite electrode pair. The cathode active material, also mixed with conductive carbon, binder, and additives is coated on aluminum foil (ca. 10–12 μm thickness) [33,36]. For NMC, NMP is currently used as solvent, with work underway to enable water-based processing [23,43]. After electrode coating, solvents are evaporated (and NMP recovered) during drying. Electrode production finishes with calendaring, slitting, and final drying [32,45], see Fig. 1.

Cell production, which requires a dry room atmosphere, consists of electrode cutting, stacking, contacting, enclosing, and filling cells with electrolyte [45]. Inactive cell material added in this segment includes cell housing, a separator which avoids short-circuits, and liquid electrolyte which enables ion-transport [33]. Cell formats include prismatic, pouch, and cylindrical cells [32]. Depending on cell format and material choice, the specific energy on cell level is between 160 and 280 Wh kg^{-1} (ref [46]).

Cell conditioning consists of formation, aging, and quality control [32,45]. The purpose of formation is that a solid electrolyte interphase (SEI), protecting the anode active material from further reduction, is formed [24,32]. The strength of charging and discharging currents during the first cycles of the LIB impacts the quality of SEI layers [24]. Industrial formation processes can take 35 hours [23]. During battery aging, cells are stored under controlled conditions for up to two weeks and monitored for non-conforming characteristics [12,23,24]. Promisingly, time for formation and aging is expected to decrease by 60–70% until 2030 [23], which reduces costs associated with capital expenditure. Approximately 15% of cells were rejected during final quality control, which at the same time could be as low as 1% by 2030 [23].

In 2015, Wood et al. [47] estimated costs for NMC_{111} cells produced in the United States as \$271 kWh^{-1}, with high contribution from electrode materials, current collectors, separator and electrode processing. Costs declined since, with recent cost models putting cells at \$106

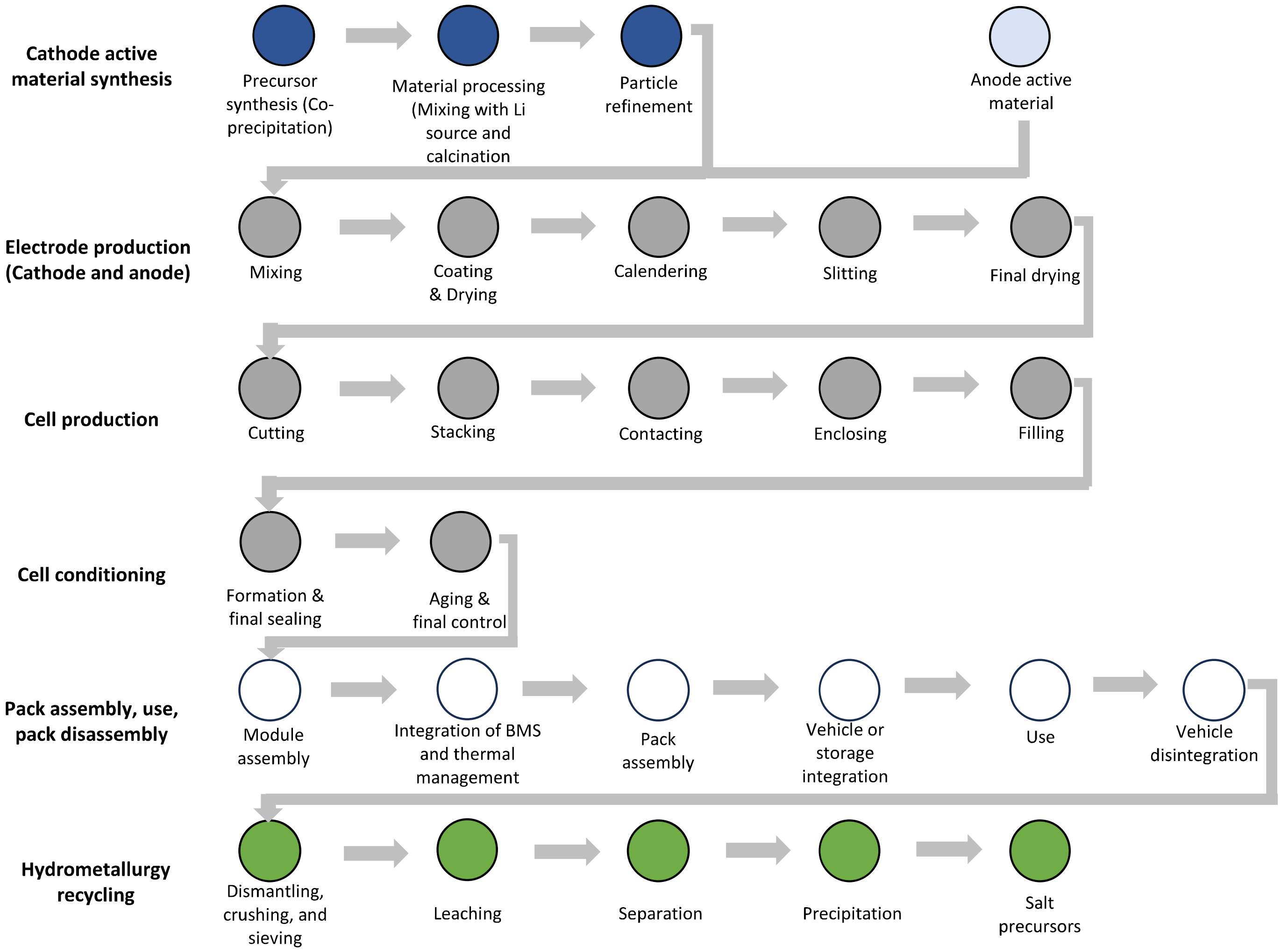

Fig. 1. Value chain of lithium-ion batteries from cathode active material synthesis to (hydrometallurgy) recycling; sources [12,32–34].

(NMC_{622}) [12] and \$98 (NMC_{811}) [11] for the production of 1 kWh cell in Europe and the United States.

Cell manufacturing in Gigafactories requires 30–50 kWh of energy (electricity and heat) to produce 1 kWh of cell capacity [48]. As with cathode active material synthesis, GWP is generally lowest in countries with high shares of low emission electricity generation. In the United States, GWP associated with 1 kWh LIB capacity, using NMC_{111} as CAM, is around 60 $kgCO_2eq$[25]. Manufacturing the same LIB in China, meanwhile, is associated with 73 $kgCO_2eq$[25]. Switching to high-nickel NMC_{811} reduces GWP by about 10%, according to ANL [25]. Crenna et al. [49] have seen an increase of 10% in GWP if NMC_{811} is used instead of NMC_{111}.

2.4. Pack assembly, use and, pack disassembly

Multiple cells are put together in modules and packs which are, fitted with a battery management system, put into electric vehicle or stationary storage applications [32,33,35]. Battery capacity for stationary storage systems range from 2 to 25 kWh in residential applications to several MWh in grid-scale storage systems [2,50,51]. In battery electric vehicles, battery pack capacities range from 15 to 100 kWh[32]. Since non-active materials such as pack housing and battery management system add weight, the specific energy of LIBs on pack level is lower than on cell level. To achieve high specific energies and low costs, LIB manufacturers aim to keep module and pack housing as light and cheap as possible. If safety requirements are met, pack designs in which cells are grouped together without modules are promising [46]. Current cell-to-pack ratios between 55% and 75% [40,46] translate to specific energies on pack level between 120 and 170 Wh kg^{-1}. Thus, the weight of a battery pack with 50 kWh is between 420 and 300 kg. Pack housing and battery management systems add between 15% and 35% to the GWP of LIB cells [49,52]. Similarly, cost calculations estimate that costs increase by 30% from cell to pack level [53]. After LIBs reach their end-of-life in mobility or stationary applications, packs are dismantled to module and cell level [35], each with distinct disassembly challenges and recovered materials.

2.5. Pretreatment and recycling

Pyrometallurgy, hydrometallurgy, or direct recycling are approaches to LIB recycling with different challenges and opportunities [35]. The level of pretreatment depends on the chosen recycling technology. Pretreatments consist of stabilization, opening, and separation based on size, density, or magnetic properties [35,54]. During stabilization, LIBs are discharged to limit potential short-circuits at later process stages [35]. Setting a suitable discharge level is crucial due to its influence on cell material properties at later recycling stages [35]. Opening of cells employs shredding or crushing technologies, usually carried out in inert gas atmosphere [35]. Physical separation technologies are used to separate black mass from other cell components such as electrolyte and current collector foils [54].

Pyrometallurgy has low standards for pre-treatment and is an established technology, but recovery of aluminum and lithium presents a challenge [35,44,54]. Commonly, alloys from pyrometallurgy are subsequently separated through hydrometallurgical treatment [54]. Hydrometallurgy has the advantage that aluminum and lithium can be recovered from waste LIBs [35]. On the other side, process maturity is slightly lower [34,35]. Leaching, separation, and precipitation form the main steps of hydrometallurgy with salt precursors such as Ni salt or Li salt as final product [28,34]. If purity requirements are sufficient, these precursor salts can be used for new cathode active material production. Inorganic acids, for example, H_2SO_4/H_2O_2, are commonly used due to a high leaching efficiency [34,35]. With these leaching agents, recovery efficiencies up to 99% and more have been achieved for Li, Ni, Mn, and Co[34]. Leaching with organic acids or bioleaching are of interest to avoid some environmental impacts associated with inorganic acids [34]. Direct recycling approaches enable a direct re-use of the cathode material as its morphology is conserved [35]. Through re-lithiation, depleted lithium is replaced [34]. Downsides of this approach are low technological readiness and high pretreatment requirements [34,35].

To reduce raw material requirements for the battery industry, recycling technologies should follow a closed-loop approach. Such a closed-loop approach requires that material properties of recycled materials are comparable to properties of virgin material [16,55]. If these requirements are met, a credit or benefit is awarded to express the positive impact of recycled material replacing virgin material [56]. Economic or environmental values of these credits depend on the costs and environmental impacts of the virgin materials that are replaced. The assumption that recycled battery materials displace virgin battery materials, with corresponding economic and environmental recycling credits, has become common practice in research on battery recycling [17,56–59].

Direct recycling and hydrometallurgy recycling of LIBs show better economic prospects than pyrometallurgy [60]. Industrial-scale hydrometallurgy recycling of NMC and NCA LIBs is profitable in the U.S., U.K., and China, with revenue from selling recycled battery-grade material higher than recycling costs [60]. At the same time, hydrometallurgical recycling of LFP LIBs is not profitable in the U.S., U.K., or China [60]. Disassembling rather than crushing LIBs before hydrometallurgical treatment has limited impact on recycling costs but disassembly increases recycling credits as more valuable cathode active materials can be recovered [61].

For cells with NMC as cathode active material, GWP associated with recycling of 1 kWh nominal cell capacity, with electricity from the European grid, was reported as 6 (pyrometallurgy), 7 (hydrometallurgy), and 8 $kgCO_2eq$ (advanced hydrometallurgy) by Mohr et al. [57] With recycling credits of 20 (pyro), 23 (hydro) and 28 $kgCO_2eq\ kWh^{-1}$ (advanced hydro), all three recycling approaches have a net-positive impact on global warming potential [57]. Recycling of LFP emits between 6 and 9 $kgCO_2eq\ kWh^{-1}$ but recovered material for replacing virgin material only gets recycling credits between 7 and 20 $kgCO_2eq\ kWh^{-1}$ (ref. [57]). Consequently, the net-benefit of recycling LFP is lower than recycling NMC. Similarly, Ciez et al. [17] report that hydrometallurgy recycling of NMC cells with the U.S. grid as source of electricity, reduces net carbon dioxide emissions. For LFP, meanwhile, credits of recycled material do not offset the carbon emissions associated with recycling of LFP cells [17]. For other environmental impact categories, recycling generally demonstrates large net-benefits related to mineral resource scarcity [57,58,62], as is indented to reduce pressure on raw-material requirements.

3. Method

3.1. System layout

The system boundary of our analysis is shown in Fig. 2. Similar to the technical background (see Fig. 1) we split the value chain in different segments. For our purpose, these include cathode active material synthesis (1), electrode production (2), cell production (3), and cell conditioning (4). Segments 2–4 are common in Gigafactories; segment 1 is a vertical upstream integration. Pack assembly, use, and pack disassembly are left out of the present analysis due to different applications and pack formats. Furthermore, the use-phase of LIBs is generally beyond the influence of LIB manufacturers (a LIB manufacturer, for example, has small influence on the intensity with which an electric vehicle is used). Due to its favourable economic and environmental perspective [17,35,57,60], hydrometallurgy recycling of cells is set as end-of-life treatment (6) and credits obtained for recycled materials subtracted from economic and environmental costs.

We assume large-scale LIB production −20 GWh per year– and LIB recycling with a capacity of 71,000 t $year^{-1}$, allowing for the recycling of cells with a nominal capacity of 20 GWh $year^{-1}$. Such a recycling facility would achieve full utilization in a future scenario where return of

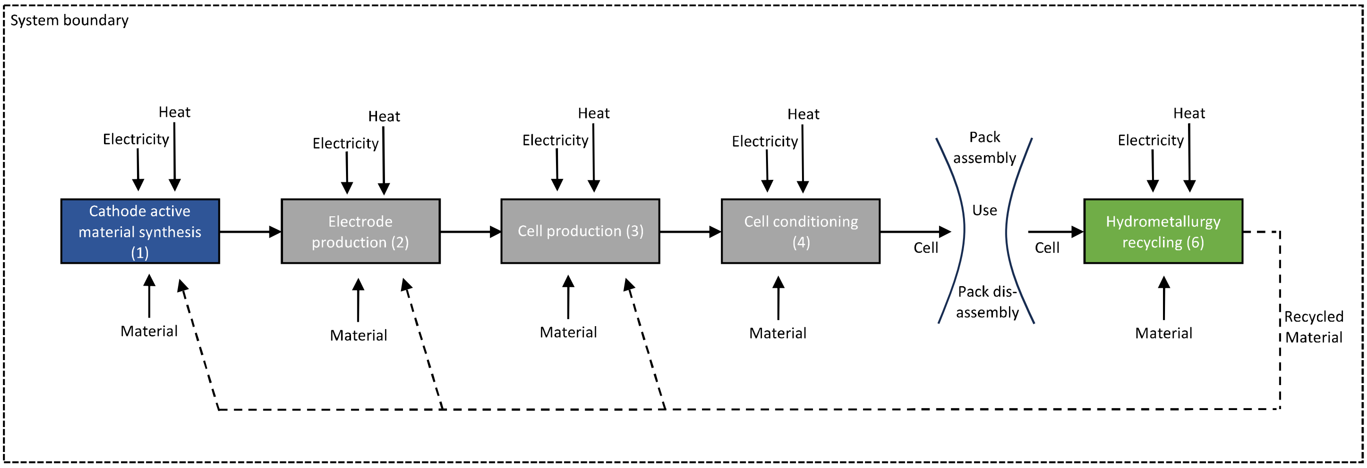

Fig. 2. System boundary and layout of analyzed value-chain segments.

end-of-life LIBs to the cell manufacturer is equal to production output. While this might not occur for some time, our analysis will address a lower utilization of the integrated recycling facility. Similar to previous research, our model applies a closed-loop recycling approach, in which recycled material serves as a substitute for virgin material with comparable quality properties and characteristics [58,62–64].

Shared technical specifications of the cell, cell production, and cell recycling are used for both cost and environmental assessments. Cell specifications are taken from the open-source CellEst 2.0 model [65,66], see Table 1. One feature of our method is that the same functional unit of 1 kWh nominal cell capacity is used throughout the whole value chain.

3.2. Cost assessment

The basic structure of the cost assessment is a process-based cost model (PBCM) approach, adapted from our earlier work [11,12]. Covering a longer value chain as well as environmental impacts meant that, compared to previous PBCMs, a higher level for definition of processes and process segments was applied.

Costs for finished cells (CAM synthesis to cell conditioning) are the sum of costs associated with each segment (Eq.1). One category are variable costs, which scale with the production volume (e.g., material and energy costs, see Eq. 2). The second cost category are fixed costs, which occur irrespective of the production volume (e.g., depreciation of buildings and equipment, Eq. 3).

We do not include costs associated with labor, maintenance and overhead. In previous work, maintenance and overhead costs have been estimated as a fixed percentage of equipment and building costs [12,17,67,68]. Estimates point to added maintenance and labour costs of 5–10% [12]. Since setting percentages for maintenance and overhead relies heavily on assumptions, potentially tilting the cost structure, we have decided to not include maintenance and overhead costs at this point. Due to the continued automation in large-scale LIB manufacturing, labor costs are expected to constitute <2% of cell costs [12]. Therefore, omitting labor costs to limit overall complexity seems reasonable.

Table 1
Technical parameters of cells, based on CellEst 2.0 model [66].

Description	Value
Cathode active material (CAM)	NMC811
Specific capacity CAM	200 mAh g^{-1}
Coating thickness CAM	100 µm
CAM – binder – conductive carbon [%]	95–2.5–2.5
Anode active material (AAM)	Graphite
Specific capacity AAM	360 mAh g^{-1}
Coating thickness anode	74 µm
AAM – binder – conductive carbon [%]	95–2.5–2.5
Cell capacity	55.8 Ah
Cell voltage	3.6 V
Cell energy	0.201 kWh
Cell format (width*height*thickness)	162*330*7 mm (Standard)
Cell weight	0.714 kg
Cell specific energy	0.281 kWh kg^{-1}

$$cost_{cell} = \sum_{p} cost^{p}_{process} = \sum_{p} \left(cost^{p}_{var} + cost^{p}_{fix}\right) \tag{1}$$

$$cost^{p}_{variable} = cost^{p}_{var,material} + cost^{p}_{var,energy} \tag{2}$$

$$cost^{p}_{fix} = cost^{p}_{fix,machine} + cost^{p}_{fix.building} \tag{3}$$

Material costs for each process are calculated by multiplying the amount of material i required for 1 kWh cell ($weight_{i,material}$) with unit costs of 1 kg material ($unit\_cost_{i,material}$), see Eq. 4. We include scrap rates to account for higher input material needs as not all process output is of sufficient quality.

$$\begin{aligned} cost^{p}_{var,material} &= \sum_{i} cost^{p}_{i,material} \\ &= \sum_{i} weight^{p}_{i,material} * unit\_cost^{p}_{i,material} * \frac{1}{1 - scrap_{p}} \end{aligned} \tag{4}$$

Most processes require energy input in form of heat and electricity. Due to the high relevance of energy input for environmental impacts, an explicit calculation of energy related cost is done for consistency. Prior cost models tended to estimate energy costs as fraction of cell costs [12,67]. Similar to material costs, energy costs for each process are obtained by multiplying heat and electricity demand ($energy\_demand_{k,energy}$) per 1 kWh cell with $unit\_costs_{k,energy}$ of heat and electricity, see Eq. 5. In our reference scenario, which is in the United States, electricity is supplied by the grid and heat for the processes by natural gas [26,40].

$$cost^{p}_{var,energy} = \sum_{\substack{k=heat,\\ electricity}} cost^{p}_{k,energy} = \sum_{k} energy\_demand^{p}_{k,energy} * unit\_cost^{p}_{k,energy} \tag{5}$$

We include equipment costs and costs for buildings. A capital recovery factor (CRF) ensures that capital costs (borrowing at interest rate r) are included (Eq. 6). Investment costs for machinery ($invest\_cost_{machine}$) and buildings ($invest\_cost_{building}$) are fitted to a 20 GWh/year production volume and 20 GWh $year^{-1}$ recycling capacity. The utilization factor ($utilization$) makes sure that fixed costs per kWh cell increase whenever production volumes are lower than the name-plate production volumes ($design\_production\_volume$), see Eq. 7,8.

$$capital\ recovery\ factor\ (crf) = \frac{interest^{*}(1+interest)^{lifetime}}{(1+interest)^{lifetime}-1} \tag{6}$$

$$cost^{p}_{fix,machine} = \frac{invest\_cost^{p}_{machine} {}^{*} crf_{machine}}{utilization^{p} {}^{*} design\_production\_volume^{p}} \tag{7}$$

$$cost^{p}_{fix,building} = \frac{invest\_cost^{p}_{building} {}^{*} crf_{building}}{utilization^{p} {}^{*} design\_production\_volume^{p}} \tag{8}$$

3.3. Life cycle assessment

Calculating environmental impacts within a standardized framework is a central motivation for life cycle assessments. As stated in ISO14040/44 [16,55], LCAs consist of for parts, which are: 1. Goal & scope definition, 2. Life cycle inventory (LCI), 3. Life cycle impact assessment (LCIA) and 4. Interpretation [16,55]. Each of the four parts is addressed subsequently. As the LCA is combined with a cost assessment, we put effort in aligning the structure of the LCA and PBCM.

Similar to the cost assessment, the goal of the present life cycle assessment is to calculate environmental impacts for cathode active material synthesis, cell manufacturing and hydrometallurgy recycling of state-of-the-art NMC_{811} LIB cells in the United States. The system boundary of the analysis, showing which process parts, energy and material flows are included, is shown in Fig. 2. In LCAs, the functional unit (FU) describes which quantifiable product or service is set as reference throughout the analysis [16,55]. We select 1 kWh of nominal cell capacity, which is the same reference as in the cost assessment, as functional unit. Life cycle inventory data, giving information about material and energy flows associated with different segments of the value chain, is gathered from technical reports, academic publications and Ecoinvent 3.8[69] as environmental database (see Tables A4 – A8 in supplementary material for further information). OpenLCA [70,71] software is used to support the implementation of the LCA.

In the life cycle impact assessment, data from material, energy and waste flows is condensed to a set of environmental impact categories. For example, emissions of CO_2, CH_4, and N_2O, all greenhouse gases, might occur along the production process. Through LCIA characterization models, these GHG emissions are transformed and condensed into CO_2 equivalents, to make results more comprehensive. Established LCIA characterization models, such as Environmental Footprint (EF) 3.0 [72–74] or ReCiPe2016 [75] capture environmental impacts in several (midpoint) impact categories. The 16 impact categories ($m = 1$–16) in EF 3.0 include, for example, *Water use*, *Resource use (minerals and metals)* and *Climate change* (see supplementary material for complete list of impact categories). EF 3.0 is used as LCIA characterization model in the present study.

Sometimes, it is difficult to relate to the absolute results in environmental impact categories. Therefore, efforts have been made to estimate the total global annual impact in each environmental impact category, for example, 55.5 billion $kgCO_2eq$ for the impact category of climate change [76]. Through normalization, which is optional according to ISO14040/44, results for each impact category ($Impact_m$) are divided by the global annual total for that impact category, provided by Crenna et al. [76] This approach gives an understanding of the relative problem that the analyzed product causes to the global total (Eq. 9). In addition to normalization, global weighting factors have been estimated for each impact category [77] to build one single score to capture the combined, relative environmental impact and support decision-making (see Eq. 10). After normalization and weighing, a combined environmental impact score (CEIS) of 1 represents the global annual total of all environmental impacts. Therefore, a CEIS value of 0.01 means that the product is responsible for 1% of all global environmental impacts. As outlined in previous work, there is merit in using a normalization and weighing approach for effective communication of environmental impacts to stakeholders [76–78]. At the same time, combined environmental impact scores should not be over interpreted. Therefore, we present global warming potential as single impact category next to combined environmental impacts, and discuss which environmental impact categories contribute most strongly to the combined environmental impact score.

$$Normalized\ environmental\ impact_{m} = \frac{Impact_{m}}{Normalization\ factor_{m}} \tag{9}$$

$$Combined\ environmental\ impact\ score = \sum_{m=1}^{m=16} Normalized\ environmental\ impact_{m} {}^{*} global\ weight_{m} \tag{10}$$

To ensure comparability with costs results, we classify environmental impacts based on the same categories as costs, that is, fixed and variable, to ensure easy comparability. In the equations below (see Eq. 11–17), which are motivated and structured similar to the cost assessment section, ***$Impact_m$*** represents each of the 16 environmental impact categories of the EF 3 LCIA characterization model. These ***$Impact_m$*** results are used to calculate normalized and combined environmental impact scores according to Eq. 9 and 10.

As no interest rate exists for calculating fixed environmental impacts associated with machinery and building, what used to be the capital recovery factor in Eq. 7,8 for costs, simplifies to 1/lifetime (***impact recovery factor***) in see Eq. 18. Going forward, one might think about whether something comparable to an interest rate could be used in the context of environmental impact assessments.

$$Impact\ result_{m,cell} = \sum_{p} Impact^{p}_{m,process} = \sum_{p} \left(impact^{p}_{m,var} + impact^{p}_{m,fix}\right) \tag{11}$$

Variable environmental impacts:

$$impact^{p}_{m,variable} = impact^{p}_{m,var,material} + impact^{p}_{m,var,energy} \tag{12}$$

$$impact^{p}_{m,var,material} = \sum_{i} impact^{p}_{m,i,material} = \sum_{i} weight^{p}_{m,i,material} {}^{*} unit\_impact^{p}_{m,i,material} {}^{*} \frac{1}{1-scrap_{p}} \tag{13}$$

$$impact^{p}_{m,var,energy} = \sum_{\substack{k=heat,\\ electricity}} impact^{p}_{m,k,energy} = \sum_{k} energy\_demand^{p}_{m,k,energy} {}^{*} unit\_impact^{p}_{m,k,energy} \tag{14}$$

Fixed environmental impacts:

$$impact^{p}_{m,fix} = impact^{p}_{m,fix,machine} + impact^{p}_{m,fix,building} \tag{15}$$

$$impact^{p}_{m,fix,machine} = \frac{invest\_impact^{p}_{m,machine} {}^{*} irf_{machine}}{utilization^{p} {}^{*} design\_production\_volume^{p}} \tag{16}$$

$$impact^{p}_{m,fix,building} = \frac{invest\_impact^{p}_{m,building} {}^{*} irf_{building}}{utilization^{p} {}^{*} design\_production\_volume^{p}} \tag{17}$$

$$impact\ recovery\ factor\ (irf) = \frac{1}{lifetime} \tag{18}$$

3.4. Filling models with data

Material input data for cathode active material synthesis, cell manufacturing, and recycling is presented in Table A4. As addressed in section 2, costs and environmental impacts of LIB production and recycling are influenced by geographic location, since, for example, local energy costs and carbon intensity of the electricity grid differ. Navigating this challenge, our first focus has been on compiling technical parameters from relevant technical reports and publications, such as energy demand for electrode processing, which are not impacted by location choice. Based on these location-independent technical parameters, local costs and environmental impacts are calculated for our reference geography in the United States.

For indicative purposes, material specific impacts for the impact category of climate change are shown alongside unit costs, see Table A4. A full set of impacts was used for calculation. For commodity materials with high price volatility, global average prices between 2020 and 2023 are used. Also, changes in highly volatile raw material prices for lithium, nickel and cobalt will be addressed in sensitivity and scenario analyses (section 3.5).

Technical data for hydrometallurgy recycling was obtained from three independent sources, identified during the literature review (see Tables A1-A3). Data from Mohr et al. [57] for a European context and Jiang et al. [59] for a Chinese location were part of life cycle assessments. Data from the often-used Everbatt model [79], built by the Argonne National Laboratory for a U.S. location, was extracted from model reports. Following our approach of extracting primarily technical data from these publications and selecting corresponding unit cost and environmental data for a U.S. reference case ensured comparability of our results (see Tables A4 – A6). As could be expected based on section 2.5., all three hydgrometallurgy recycling processes share that input of H_2SO_4, NaOH and Na_2CO_3 is central. Material recovery rates are shown in Table A5, and generally exceed 90% for high value materials such as lithium, nickel, cobalt, and copper. Process specific energy requirements for all parts of the value chain are shown in Table A6. We assume energy costs of \$0.08 kWh^{-1} (electricity) [80] and \$0.015 kWh^{-1} (natural gas) [81] for the United States. Based on the U.S. electricity mix of 2022, our LCA leads to GWPs of 0.45 $kgCO_2eq\ kWh^{-1}$ (electricity) and 0.21 $kgCO_2eq\ kWh^{-1}$ (heat, natural gas).

Previous work has shown that minimum equipment costs converge to an optimum for large-scale LIB manufacturing [11]. Above an annual production volume of 10 GWh $year^{-1}$ for NMC_{811} cells, costs for cell manufacturing tend to remain stable because economies of scale have reached full potential. We assume an equipment lifetime of 6 years [67] and a discount rate of 10%. Cost data for recycling equipment is scarce. Therefore, generic equipment costs for an industrial hydrometallurgy recycling on LIBs [82] are used for all three recycling processes, see Table A7.

Commonly, depreciation of building accounts for <1% of total cell costs [12]. High level floor requirements for cell production and recycling were adapted from Chordia et al. [26] As a Gigafactory with 16 GWh $year^{-1}$ needs 150,000 m^2 of factory building, of which 75% is used for cell production and 25% for recycling, we scale the floor requirement to fit a production volume of 20 GWh $year^{-1}$, see Table A8. Within the cell production process, we assume for simplicity that each of the four segments requires a comparable level of floor space and building costs of \$3000 m^{-2} (ref. [67]). Due to limited life cycle inventory data for battery manufacturing machinery, building and equipment are together modelled on a general electronics factory (cell manufacturing) and precious metal factory (recycling), following the example of Chordia et al. [26] Lifetime of building is set to 25 years [26].

3.5. Sensitivity and scenario analyses

To address uncertainty in key technical, cost, and environmental parameters, we conduct a sensitivity analysis. An upfront sensitivity gives a perspective on the most influential factors. Also, our method should support decision-makers in comparing different strategic scenarios. In the scenario analysis, our goal is to demonstrate how fellow researcher or practitioners can adjust our approach to improve their combined value generation across the battery value chain.

Evaluated scenarios are:

1. Use of wind power and electric heating instead of U.S. grid electricity and natural gas. Levelized cost of electricity from wind power are estimated as \$60 MWh^{-1} (ref. [83]). Intermittency problems associated with wind power are left out at this point.
2. Decreased scrap rate of each process segment from 5% to 1%.
3. Volatility in raw material prices for nickel, lithium, and cobalt using highest prices in period between 2020 and 2023 rather than average prices (see Table 2).
4. Lower utilization (10% vs. 90%) of recycling facility.

4. Results/discussion

4.1. Cell manufacturing

The relative contribution of materials, energy, equipment, and building to cell costs, CO_2 emissions and the combined environmental impact score is shown in Fig. 3, The cost assessment finds cell costs, without labour, maintenance and overhead of \$94.5 kWh^{-1}. The LCA shows a global warming potential of 64.5 $kgCO_2eq\ kWh^{-1}$ and a combined environmental impact of 4.0×10^{-12} kWh^{-1}. Zooming in on combined environmental impacts, Fig. 4 shows that the combined environmental impact score is a result of the negative effect of LIB manufacturing on *Ecotoxicity (freshwater)*, *Reosurce use (minerals and metals)*, *Eutrophication (freshwater)* and *Climate change*. Summing up the bars of all environmental impact categories in Fig. 4 leads to the stated combined environmental impact score of 4.0×10^{-12} kWh^{-1}. A high contribution to *resource use (minerals and metals)*, of the raw materials copper, nickel, and cobalt, is responsible for the outsized share of these three materials in combined environmental impacts. The impact category of *Resource use (minerals and metals)* aims to capture the scarcity of minerals by calculating a factor between the world annual production of a material and global material reserves [85,86]. Levels of annual copper mining are high compared to global copper reserves, leading to comparably high impacts in *Resource use (minerals and metals)* for 1 kg of copper [85]. The impact category of *Ecotoxicity (freshwater)* addresses the adverse effects of toxic materials on aquatic ecosystems [86,87]. Here, emissions of toxic materials during open-pit mining account for much of the *Ecotoxicity (freshwater)* associated with nickel and copper [69].

Material accounts for 69% of cell costs. On a process level, \$45 or almost half of cell costs are locked in during cathode active material synthesis (see Fig. 5). This underlines the necessity to include CAM synthesis as part of the value chain in cost models. With depreciation of equipment (\$23.4) and building (\$2.8) responsible for 28% of cell costs, LIB manufacturing is a capital-intensive business. Interestingly, costs for electricity (\$3.2) and heat (\$0.4) are relatively small compared to material and equipment costs. Although less important for overall costs, the LCA shows that energy consumption is of high relevance for the GWP of cells. Consumption of electricity during CAM synthesis and cell manufacturing accounts for 28% of total GWP, with another 8% coming from burning of natural gas for process heat (see Fig. 3 and Fig. 5).

With a GWP of 17.8 $kgCO_2eq\ kWh^{-1}$ associated with electricity consumption, using low-carbon energy sources presents an opportunity to reduce GWP. CAM synthesis and electrode production are the process segments with the highest share on costs, GWP and environmental impacts (see Fig. 5). Thus, integrating CAM synthesis into Gigafactory layouts allows companies to control not only costs, but also

Table 2
Variation in raw material prices for nickel, cobalt and lithium; source [84]:.

$Material_i$	*unit_cost* [\$ kg^{-1}]		
	Average	Low	High
$NiSO_4$	7.8	6	12
$CoSO_4$	11.2	11	30
LiOH	25.4	5.6	39

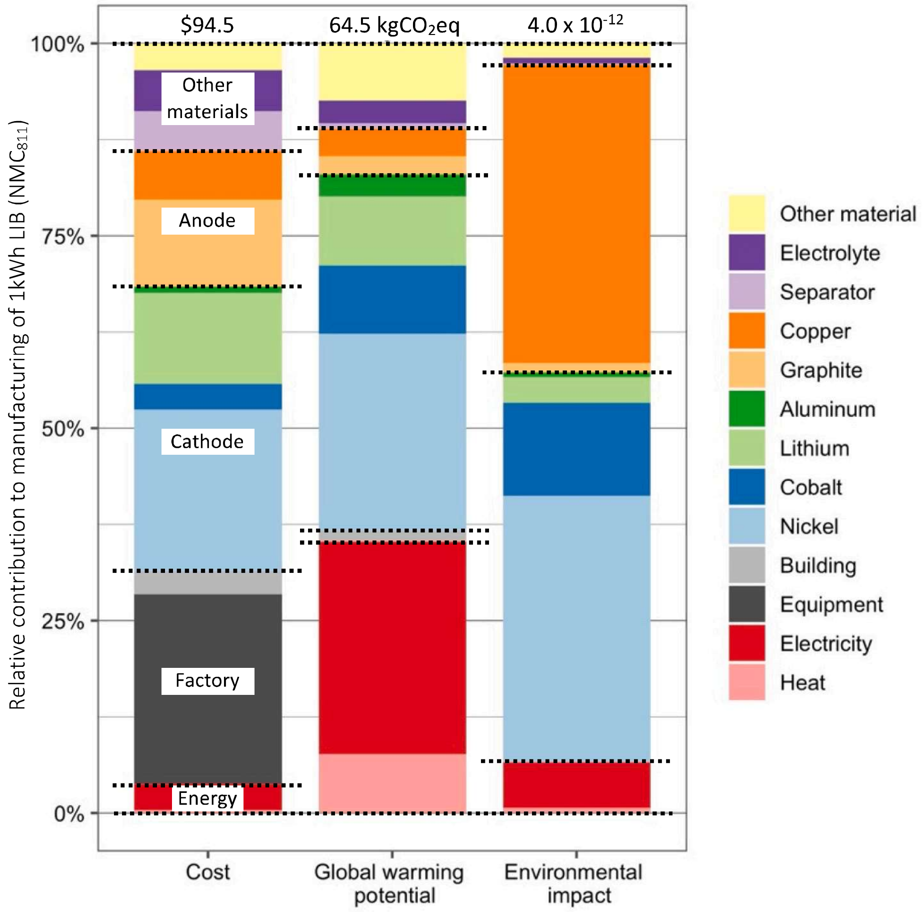

Fig. 3. Relative contribution of material, energy, equipment and building to costs, GWP and combined environmental impact score for the production of NMC$_{811}$ LIB cells.

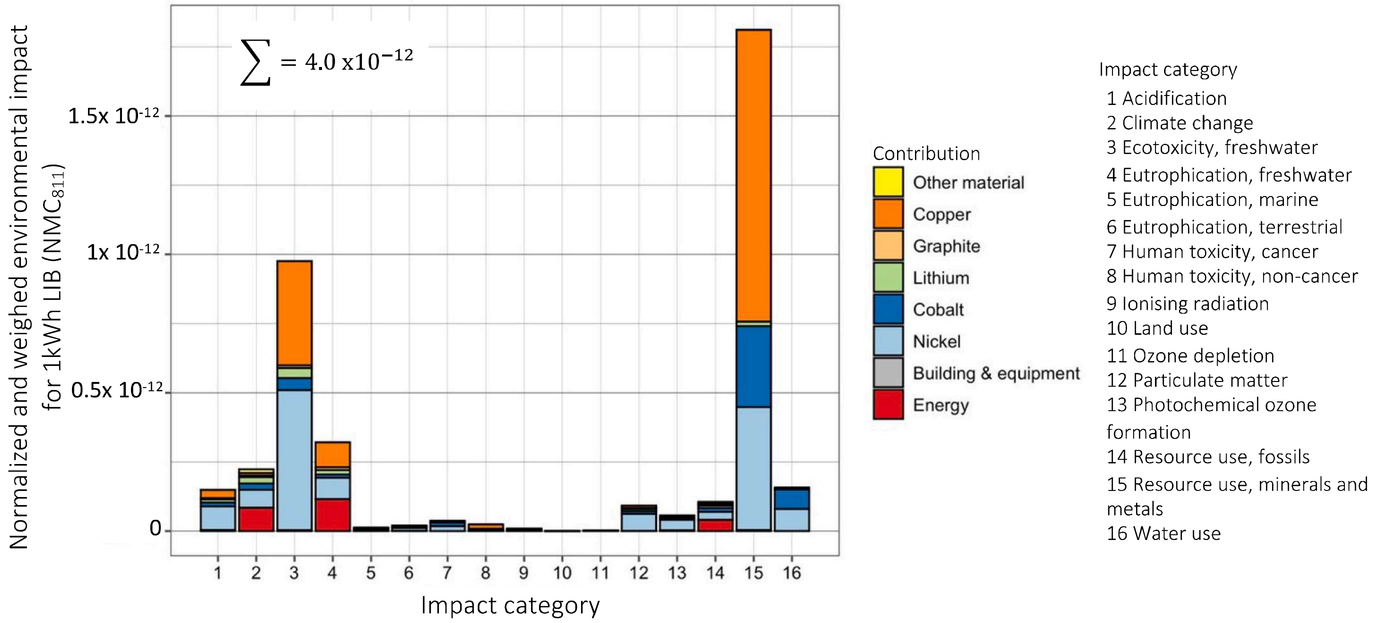

Fig. 4. Detailed contribution analysis of normalized and weighed environmental impacts.

environmental impacts. At the same time, further upstream integration into nickel, cobalt and copper mining might be a promising objective for LIB manufacturers to increase control from an overall environmental viewpoint.

In the present study, costs for NMC$_{811}$ cathode active material are around \$36/kg which is higher than the \$21.5 kg^{-1} (NMC$_{811}$) in Ahmed

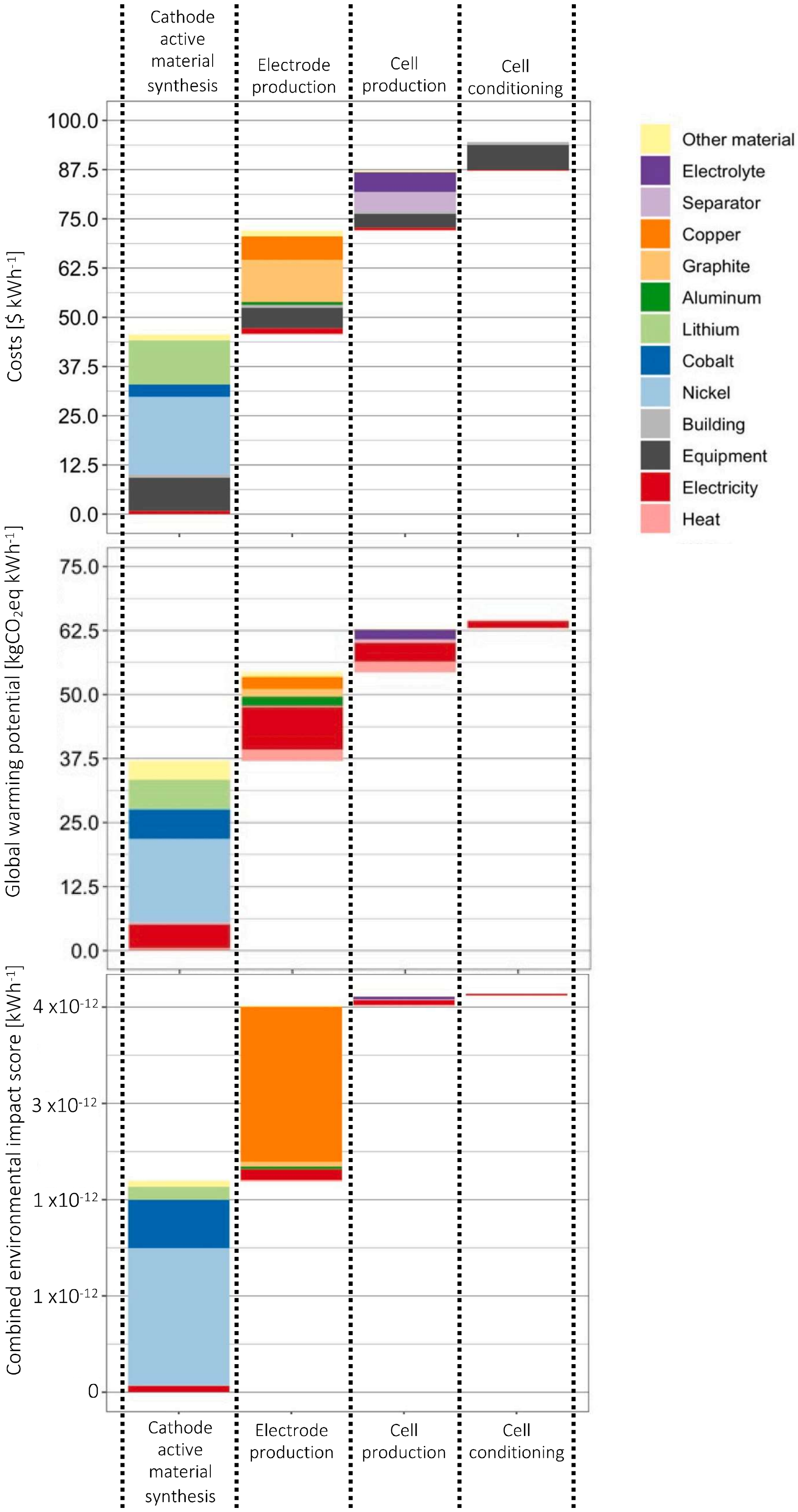

Fig. 5. Contribution of process segments to costs, GWP, and combined environmental impacts for NMC_{811} LIB cells.

et al. [38], and a result of increased raw material prices. With 21 $kgCO_2eq\ kg^{-1}$, the GWP of NMC_{811} falls between the 16 $kgCO_2eq$ for synthesis of NMC_{111} in the U.S. [25,40] and 32 $kgCO_2eq$ in China [41]. On a cell level, our calculated cell costs of \$94.5 kWh^{-1} are quite similar to the \$98 kWh^{-1} reported by Mauler et al. [11] for NMC_{811} cell production in Europe or the United States. A GWP of 64. $kgCO_2eq$ is 30% higher than the 50 $kgCO_2eq$ in Chordia et al. [26] with low-carbon energy but lower than 104 $kgCO_2eq\ kWh^{-1}$, for a production in South Korea. GWP associated with 1 kWh of LIB and NMC_{811} as CAM, is around 55 $kgCO_2eq$ in the United States in Winjobi et al. [25], which is 20% lower than our results. Previous work has not yet used a normalized and weighted environmental impact score but similar to the present findings, a high contribution of nickel, cobalt and copper to mineral resources scarcity has been found [26,88]. Researchers can incorporate their own material, cost, and environmental input data into the presented method to calculated combined environmental and economic results for their battery technology, location, or value-chain layout.

4.2. *Cell recycling*

Costs, GWP, and combined environmental impacts associated with hydrometallurgical recycling of NMC_{811} cells are shown in Fig. 6. We differentiate three sources of process descriptions for the hydrometallurgy recycling process [57,59,79], see also supplementary information. In the United States, our cost assessment finds that recycling cells with a nominal capacity of 1 kWh –the useful capacity of a battery at end-of-life is usually between 60 and 80% of nominal capacity– costs \$6.8 to \$8.6. These costs are fairly small compared to cell manufacturing costs of \$94.5 kWh^{-1}. Global warming potential associated with recycling is between 4.0 and 5.8 $kgCO_2eq\ kWh^{-1}$, depending on the process design, compared with 64.5 $kgCO_2eq$ for cell production. Variation between the three hydrometallurgy processes is less than \$2 and 2 $kgCO_2eq\ kWh^{-1}$ cell capacity, indicating some alignment. Combined environmental impact scores are 0.6×10^{-13} to 1.2×10^{-13} kWh^{-1}, which is <3% of the combined environmental impact associated with cell manufacturing in Fig. 3.

During recycling, depreciation of equipment is responsible for \$3.4 kWh^{-1}, which is lower than the depreciation of equipment used for CAM synthesis (\$8.4 kWh^{-1}). In all three recycling processes, consumption of sulfuric acid is responsible for 18% to 21% of total costs, see Fig. 6. Similar to cell manufacturing, energy consumption contributes little to costs (1–5%) but substantially to global warming potential (15–38%).

Before turning to recycling credits and a discussion of the whole value chain, it is sensible to briefly address the sensitivity of results. Fig. 7 shows the impact on costs and GWP of a 30% increase or 30% decrease in key parameters, such as electricity demand, electricity cost, carbon intensity of electricity or interest rate. If nickel costs were to fall by 30%, this would reduce cell costs by \$6 kWh^{-1}, see Fig. 7. Using average European electricity costs of \$0.18 kWh^{-1} (ref. [89]) in 2022 for non-residential households increases cell costs by \$3 kWh^{-1}. At the same time, lower average carbon intensity of European grid electricity (0.31 $kgCO_2eq\ kWh^{-1}$) compared to the U.S. (0.45 $kgCO_2eq\ kWh^{-1}$) reduces GWP associated with cells by 5.4 $kgCO_2eq\ kWh^{-1}$. Naturally, a comparable level in GWP reduction is achieved if electricity demand is decreased by 30%. Compared with lower carbon intensity, however, a reduced electricity demand has the added benefit of bringing down costs by \$1 kWh^{-1}. Assuming an interest rate of 7% instead of 10% reduces cell production costs by \$2.7 kWh^{-1} and recycling costs by \$0.5 kWh^{-1}.

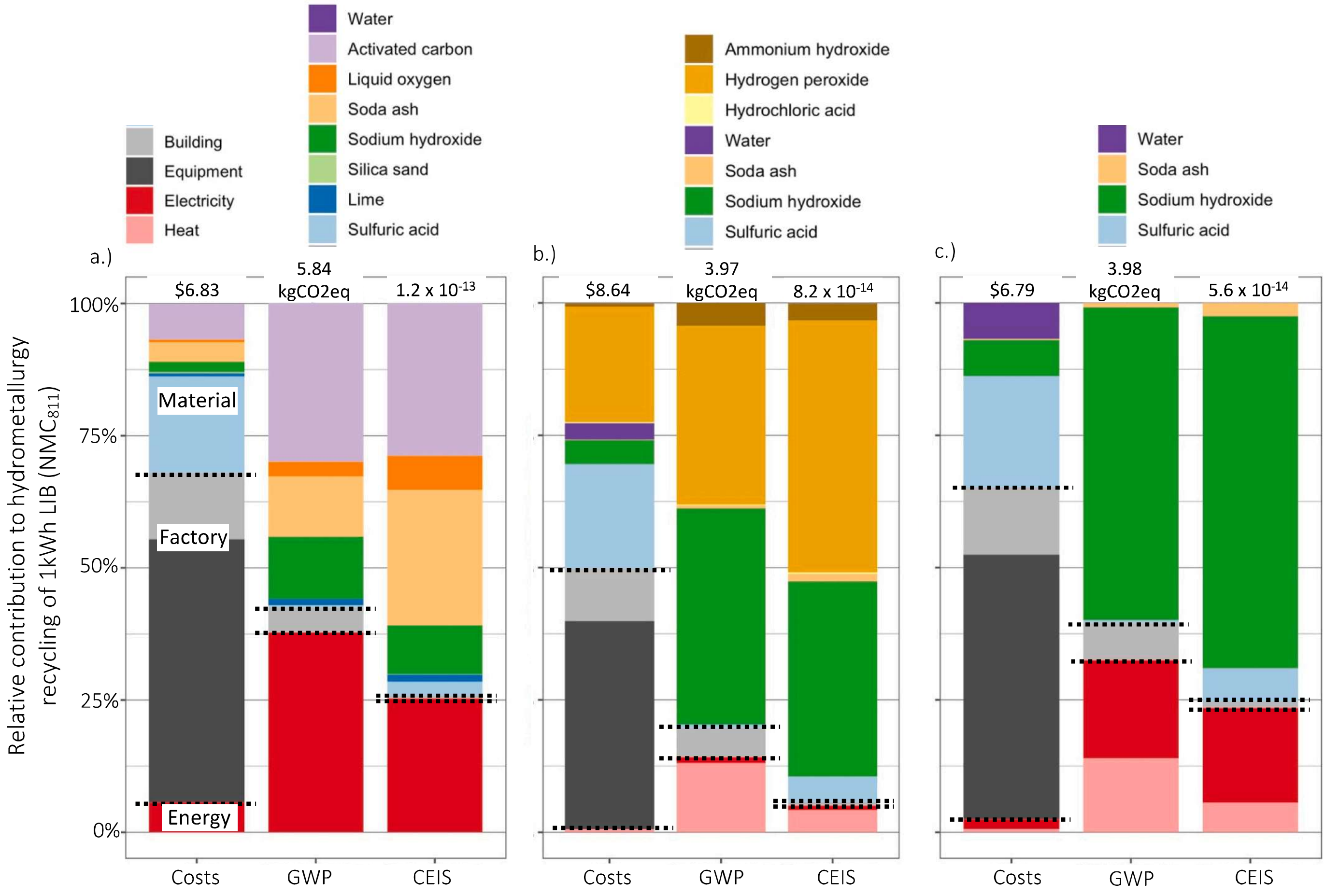

Fig. 6. Relative contribution of material, energy, equipment and building to costs, GWP and combined environmental impact score (CEIS) for recycling of 1 kWh NMC_{811} cells with process data based on: a.) Mohr et al. [57], b.) ANL Everbatt [79], c.) Jiang et al. [59]

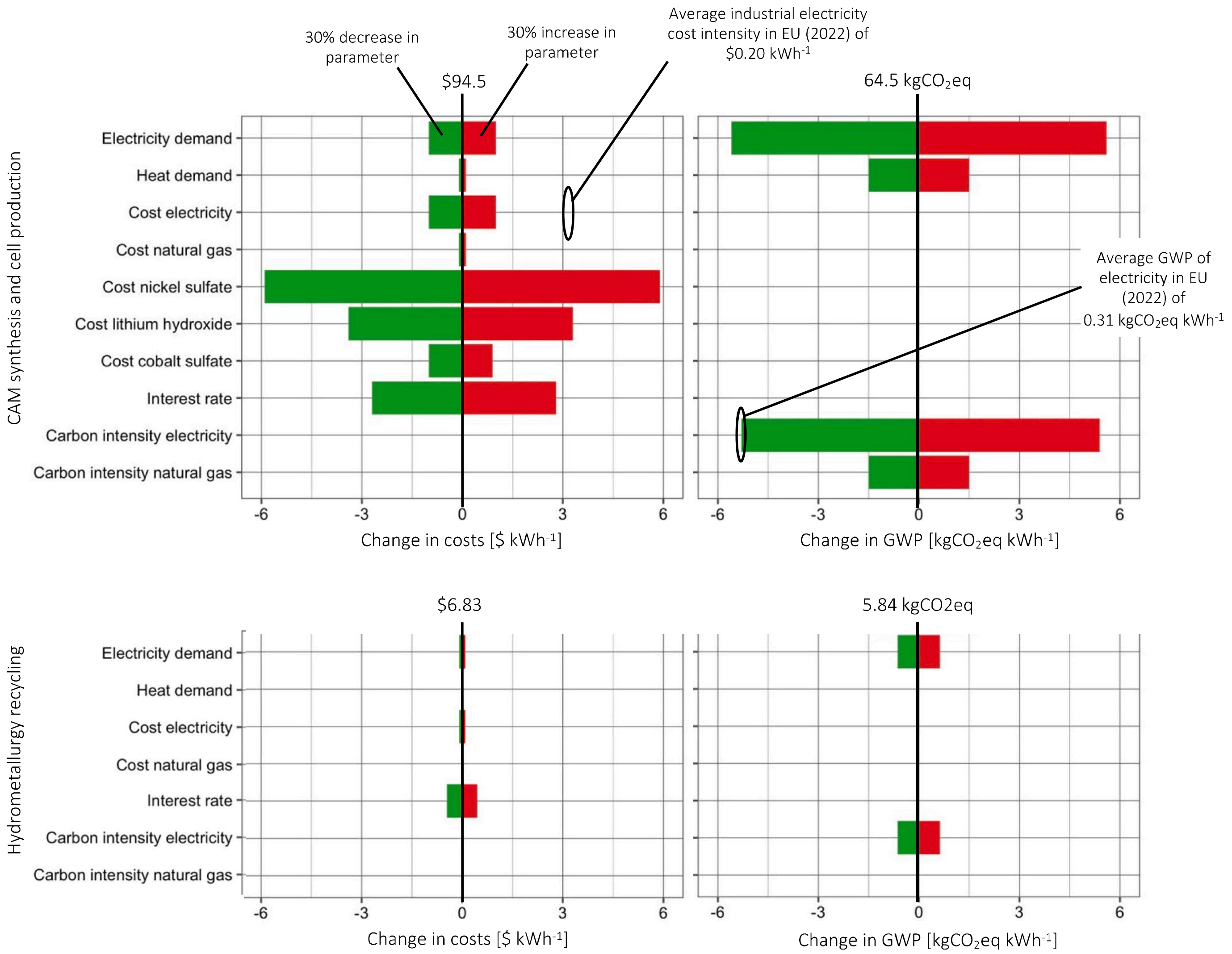

Fig. 7. Sensitivity analysis.

As outlined in section 3, material recovered in the recycling process substitutes the use of new virgin raw material. The recovery rate specifies which fraction can be recovered of a given material put through the recycling process. Combining the evaluation of recycling processes with an analysis of the upstream cell production allows to identify promising recycling targets from both costs and environmental angles. Based on the analysis of cell production, one could, for instance, expect recycling of graphite to be helpful in reducing cell costs, but less suited to reduce GWP of cells. In sum, we expect high recovery rates for lithium, cobalt, nickel, and graphite as central for economic credits.

Economic and environmental credits awarded to the recycling of 1 kWh NMC$_{811}$ cells are shown in Fig. 8, with material recovery rates of each process stated for convenience (see also Table A5). Without recycling of scrap material, which occurs during the cell production, economic credits of recycled material are \$30 to \$48 kWh^{-1}. If waste material scrap of the cell production was also recycled, credits would increase to \$36 to \$56 kWh^{-1}. Thus, recycling of scarp material next to end-of-life cells adds up to 25% of credits per kWh nominal cell capacity. The process based on Mohr et al. [57] achieves highest economic credits of \$48 without and \$56 with scrap recycling due to high recovery rates. These high recovery rates are, at the same time, responsible for highest credits in GWP of 30 kgCO$_2$eq kWh^{-1} without and 35 kgCO$_2$eq kWh^{-1} with scrap recycling.

For cell manufacturing, nickel, cobalt, and copper have accounted for >83% of combined environmental impacts. Therefore, high recovery rates for these three materials ensure that much recycled material can substitute virgin raw material. This substitution leads to substantial credits in combined environmental impact scores of up to 3×10^{-12} kWh^{-1}. Compared with the costs and environmental impacts of the recycling process, the credits obtained for recovered material far outweigh the costs and environmental burdens. Failed recovery of graphite in the process based on Jiang et al. [59] limits the upside potential for economic credits.

Our cell recycling costs are lower than the \$12 kWh^{-1} for hydrometallurgy recycling in the United States reported by Lander et al. [60] The costs for materials used during the hydrometallurgy recycling are around \$3 kWh^{-1} in Lander et al. [60], which is in good alignment with material costs between \$2.2 kWh^{-1} and \$4.3 kWh^{-1} in our analysis, but overhead costs are higher. Overall, our results confirm the findings of prior work [18,57,58,60,63] that economic and environmental credits awarded for hydrometallurgy recycling outweigh economic and environmental burdens associated with the cell recycling process. Compared with Mohr et al. [57], whose technical description served for one of the hydrometallurgy processes, our results of 5.8 kgCO$_2$eq are lower than the 8 kgCO$_2$eq stated for recycling of NMC$_{111}$ LIBs. The discrepancy is, in part, explained by differing assumptions about the specific energy of the cells. With 170 Wh kg^{-1}, the specific energy of NMC$_{111}$ cells in Mohr et al. is about 40% lower than the 280 Wh kg^{-1} in the present work. In good alignment with previous work, our results show that recycling reduces impacts in *mineral resource scarcity* by up to 75% [57,62].

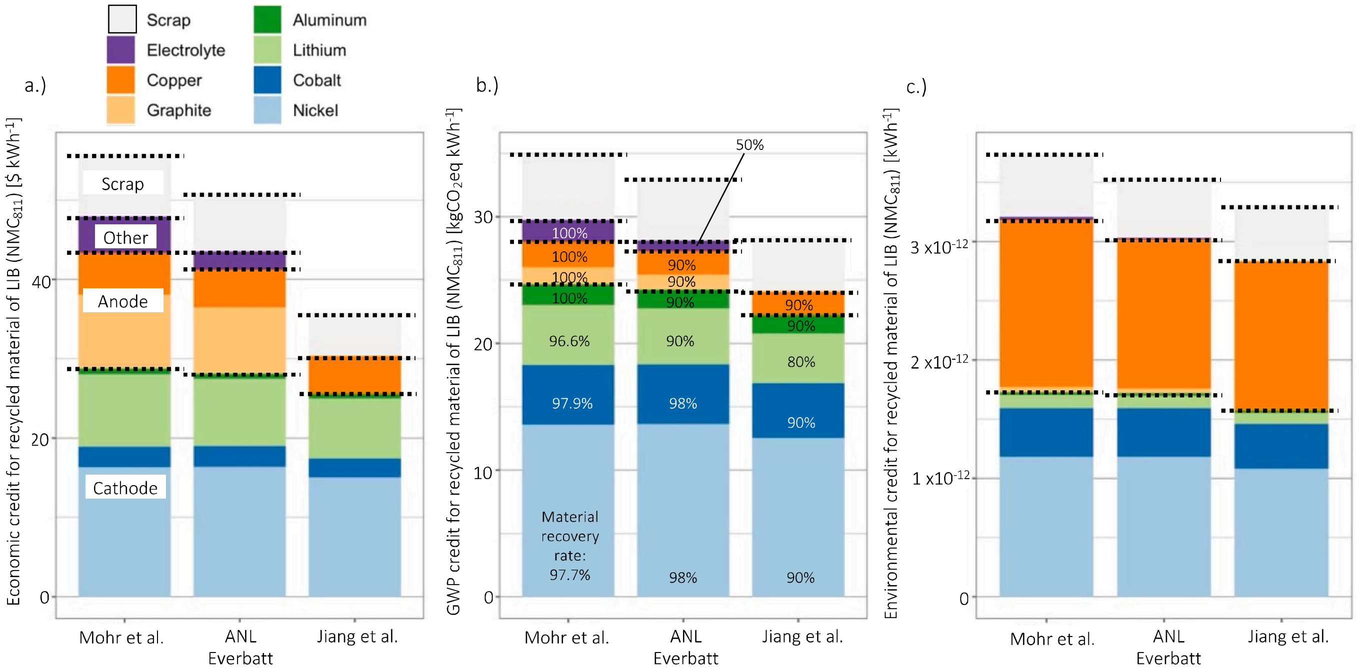

Fig. 8. Credits awarded to recycled/recovered material from recycling of 1 kWh NMC_{811} cells for a.) costs, b.) GWP, and c.) combined environmental impact scores.

4.3. Combined evaluation approach

Guiding decision-makers with a comprehensive overview of costs and environmental impacts across several parts of the LIB value chain is another objective of this work. Going forward, we present a comprehensive dashboard to support stakeholders. Visualization of process steps in Fig. 9 match the product system presented in Fig. 2. The hydrometallurgy recycling process of Mohr et al. [57] is used in Fig. 9. The break between cells leaving cell conditioning and start of the recycling demonstrates again that pack assembly, use, and pack disassembly were left out of the present analysis. Based on pack design and application, cell manufacturers could adapt the presented dashboard to include additional parts of the value chain.

Cells leaving final quality control during cell conditioning are set as the baseline for cost and environmental comparisons. In practice, a cell manufacturer could sell cells to automotive original equipment manufacturers (OEMs), and get the cells returned after they reached end-of-life. In line with Fig. 3, costs of \$94.5, GWP of 64.5 $kgCO_2eq$, and combined environmental impacts of 4.0×10^{-12}, represent 100%. As is seen quickly in Fig. 9, 52% of environmental impacts and 48% of costs are associated with CAM synthesis. Electrode production adds more to environmental impacts (44%) than to costs (28%). Cell conditioning, on the other side, accounts for 8% of total cells costs but only a much smaller fraction of GWP (2%) and environmental impacts (<1%).

Putting end-of-life cells through recycling adds to cell costs (7%), GWP (9%) and environmental impacts (3%). Compared to the recycling credits obtained for the substitution of virgin material by recycled material, the added burden of the recycling process seems reasonably small. After recycling credits have been accounted for, total costs of the cell come down by 32% (without scrap material recycling) and 44% (with scrap material recycling). Overall benefits for combined environmental impacts are even higher. As most of the combined environmental impact of cells is associated with materials, notably, copper, nickel, and cobalt, recovering critical raw materials reduces overall environmental impacts of cells by 67–73%. Relative benefits of recycling for GWP are smallest, with reductions of 23–38%. This is explained by the high share of energy related CO_2eq emissions. These emissions, for example, associated with repeated charging and discharging during cell conditioning, cannot be reversed through recovery of materials.

In effect, based on the reference system layout, applying hydrometallurgy recycling to end-of-life cells has highest potential to limit combined environmental burdens. For mitigation of GWP associated with cell production, recycling is not as efficient. In this respect, the proposals of the European Commission to require minimum targets of recycled battery material [90] might be better suited for achieving a closed-loop value chain because encouraging closed-loop recycling through strict targets for GWP is less suitable. From an economic perspective, recycling of cells is beneficial.

4.4. Employing the dashboard to strategic scenario analysis

The comprehensive eco-environmental dashboard shows how adjustments along the process route influence costs, GWP, and environmental impacts. While four scenarios are evaluated in the present work, no limits exist to the design of additional scenarios. Small bars in Fig. 10 represent the baseline situation, with the standardization to 100% introduced in Fig. 9. Starting from there, adjusted results are represented by wide bars.

Wind power is used instead of U.S. grid electricity and natural gas to fulfill energy requirements in scenario 1. Resulting from the small share of energy costs on total costs, changing the energy source has limited effect on total costs throughout the value chain. Combined environmental impacts are only marginally reduced (−4%). Substantial benefits, however, are achieved towards a reduction of GWP. Greenhouse gas emissions along the value chain are reduced by 33%. Energy intensive process segments, such as electrode production, benefit most from changing the energy source to low-emission alternatives. GWP of cells leaving cell conditioning is now lower than for cells which have gone through recycling in the baseline scenario, further strengthening the argument that changing the energy source is a more convenient way to reduce CO_2 emissions associated with LIBs rather than recycling. For decision-makers, scenario 1 outlines a path towards low carbon footprints of cells with limited effect on other environmental impacts and costs.

Bringing down scrap rates from 5% to 1% (scenario 2) reduces costs, GWP and combined environmental impacts by 10%. Reduction in GWP of cells is less than the 33% reduction achieved in the first scenario. On the other side, the comprehensive nature of the dashboard allows to spot

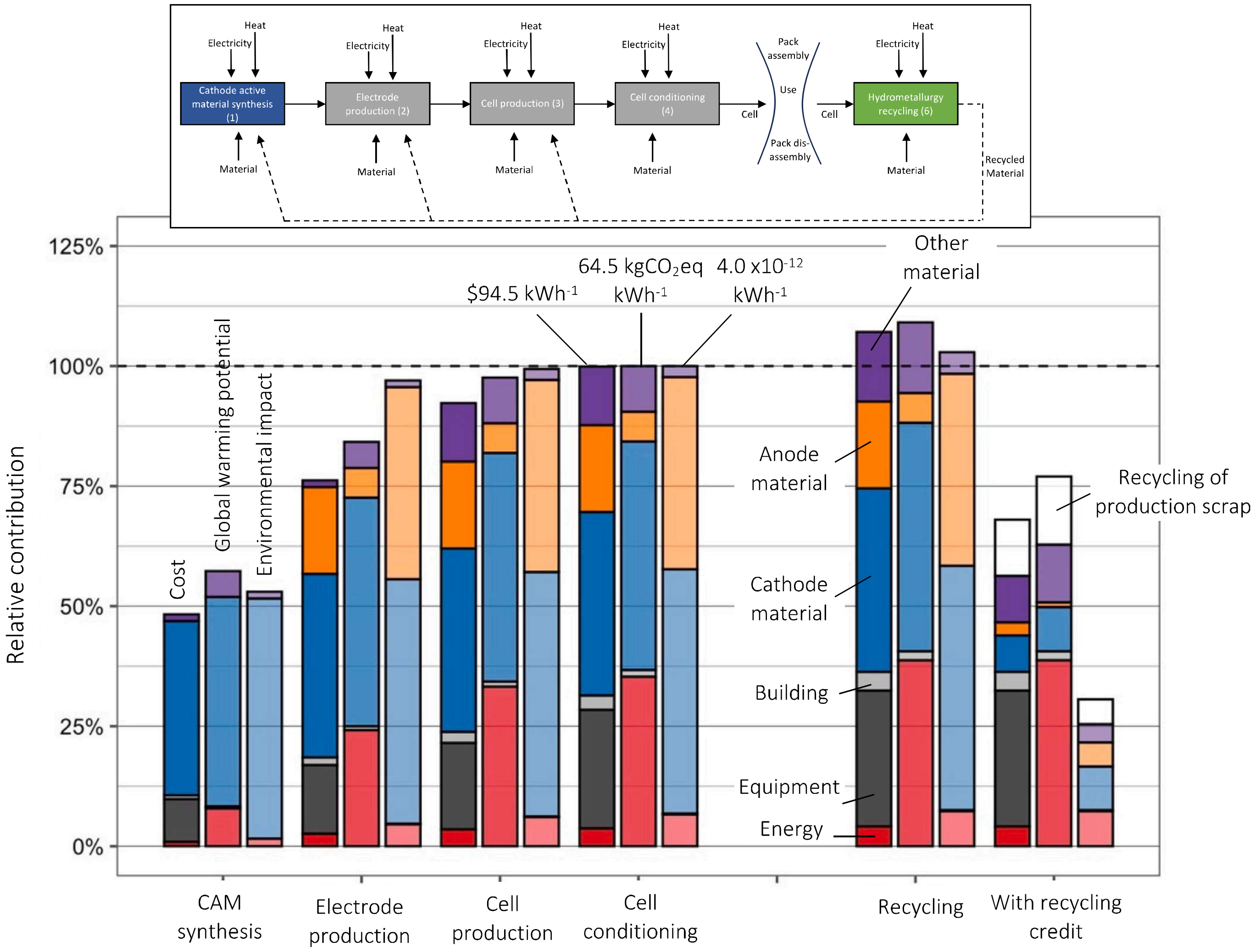

Fig. 9. Integrated value-chain dashboard for NMC_{811} cells.

added benefits for costs and combined environmental impacts which are much larger than in scenario 1. Thus, putting resources towards the achievement of scenario 2 provides a path towards lower costs, CO_2 emissions and environmental impacts.

Raw material costs are subject to market volatility (and a high sensitivity of costs to nickel prices was seen in Fig. 7). Therefore, the third scenario represents the impact of cost increases for nickel, lithium, and cobalt. Differing from the previous two scenarios, increasing raw-material costs only influence costs but not GWP or environmental impacts, see Fig. 10. Also, higher raw material prices increase the economic credit awarded to recycled material. Consequently, integrating a recycling facility into LIB Gigafactories limits exposure to rising raw material costs.

In practice, cell manufactures are faced with a situation in which their recycling capacity will have a low utilization. This is due to the temporal difference between the point at which cells are placed on the market and the point at which cells reach end-of-life. With a utilization of 90%, the annual output of the Gigafactory is 18 GWh $year^{-1}$. A reduced utilization of 9% is thus corresponding to 1.8 GWh $year^{-1}$ of recycled cells. A low utilization of the recycling facility increases the depreciation of building and equipment for recycling cells. In addition, GWP and combined environmental impacts increase slightly. The credit for recovered material, meanwhile, remains the same. But it has to be considered that in such a scenario only 10% of produced cells will benefit from recycling credit offsets.

The selected scenarios cover only a fraction of possible options. Thus, industry practitioners are encouraged to include additional scenarios and support their decision-making based on comprehensive cost and environmental insight provided by the value-chain dashboard.

5. Conclusion

Rapidly growing demand for lithium-ion batteries, cost pressure, and environmental concerns with increased production of batteries require comprehensive tools to guide stakeholders' decision-making. To date, little research has assessed economic and environmental assessments at the same time across production and recycling of LIBs. The present work addressed this short-coming by providing a state-of-the-art cost assessment and life cycle assessment, covering the value-chain segments of cathode active material (NMC_{811}) synthesis, cell manufacturing and hydrometallurgy recycling. Costs, global warming potential and combined environmental impacts were calculated for cell production as well as recycling, using the same underlying cell and process parameters gathered through a comprehensive review of academic and industrial literature. To increase transparency, input parameters, alongside corresponding sources are explicitly stated throughout the work. Further, we contribute a comprehensive dashboard to provide cost, GWP and environmental impacts across the process segments.

Excluding labor, maintenance, and overhead costs, we calculate cell costs of \$94.5 kWh^{-1} for large-scale cell manufacturing, and an additional \$6.8 to \$8.6 kWh^{-1} for end-of-life recycling. With high recovery rates for nickel, lithium, cobalt, graphite, and copper, credits for

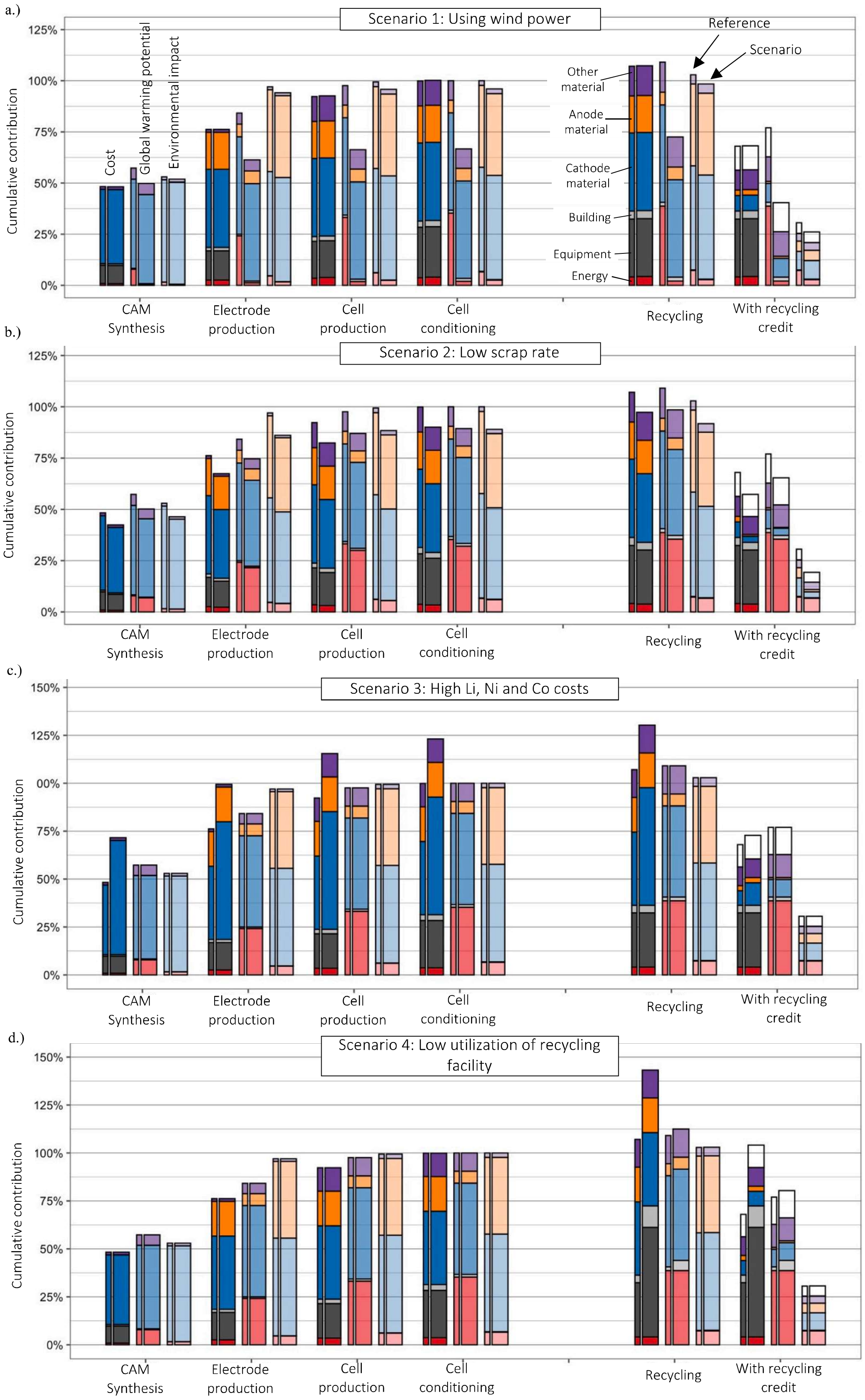

Fig. 10. Scenario analysis with integrated value-chain dashboard for a.) use of wind power, b.) low scrap rate, c.) high raw material costs, and d.) low utilization of recycling facility.

recycled raw material can offset up to half of material costs. This is especially true whenever scrap material from the cell production is also subject to recycling. In line with previous results, we find a high contribution of material costs to overall cell costs, with cathode active material synthesis as the most expensive process segment. The LCA estimates global warming potential of 64.5 $kgCO_2eq\ kWh^{-1}$ for cell production in the United States. Shifting manufacturing to Europe will likely increase costs by 5% due to higher energy costs. While high-cost materials, such as nickel, cobalt and lithium also contribute substantially to overall GWP, energy used during the production process is responsible for almost half of GWP. Hydrometallurgical cell recycling adds another 4.0 to 5.8 $kgCO_2eq$ to GWP. Normalized and weighed environmental impacts are $4 \times 10^{-12}\ kWh^{-1}$. Most of this aggregated environmental impact figure comes from *Ecotoxicity (freshwater)* and *Resource use (minerals and metals)* associated with copper, nickel, cobalt, and lithium raw material extraction. Put into context, $4 \times 10^{-12}\ kWh^{-1}$ means that producing 1000 GWh of cells would roughly be responsible for 0.4% of total global environmental impacts. Compared with costs and GWP, recycling brings most benefit to the combined environmental impacts.

A limitation of the present work is the exclusion of pack assembly, use-phase, and pack disassembly as part of the value-chain. Based on previous work, both costs and GWP might increase by 20 to 35% if 1 kWh of LIB on pack level rather than cell level is set as reference [49,52,53]. In addition, environmental data for raw materials relies on Ecoinvent 3.8 data, which is not always as up to date as some recent LCAs for specific raw materials such as lithium [91–93]. Hydrometallurgy recycling was selected due to high availability of data, and a generally better cost and environmental performance compared to pyrometallurgy. But direct recycling is a promising technology which recovers the cathode active material and should be included in subsequent work.

In sum, the present work has shown that cathode active material synthesis remains a crucial process segment for both economic and environmental reasons. Cost and environmental burdens associated with the hydrometallurgical recycling process remain small compared to the upside benefits. Integrating recycling facilities, even at low utilization levels, into Gigafactories allows to hedge against volatility in raw material prices. Use of low-carbon energy throughout the cell manufacturing process helps to bring GWP down. However, broader environmental impacts cannot be reduced this way. For reducing combined environmental impacts, low scrap rates and recycling are vital. Providing a balanced economic and environmental look for the battery industry will, as for other industries, become more crucial as legislation and society demand measures to make the global economy more sustainable. Despite some limitations, establishing the simultaneous assessment of cost and quantified environmental impacts as new standard for industrial production and recycling processes, which is not limited to the battery industry, is hoped to take inspiration from the present work.

Funding

This research did not receive any specific grant from funding agencies in the public, commercial, or not-for-profit sectors.

CRediT authorship contribution statement

Moritz Gutsch: Visualization, Methodology, Investigation, Formal analysis, Data curation, Conceptualization, Writing - original draft, Writing - review & editing. **Jens Leker:** Validation, Supervision, Conceptualization.

Declaration of Competing Interest

The authors declare that they have no known competing financial interests or personal relationships that could have appeared to influence the work reported in this paper.

Data availability

The authors declare that the data used as model inputs supporting the findings of this study are available within the paper and its Supplementary Information files. Additional questions about the data supporting the findings of this study can be directed to the corresponding author.

Appendix A. Supplementary data

Supplementary data to this article can be found online at https://doi.org/10.1016/j.apenergy.2023.122132.

References

[1] Brodnicke L, Gabrielli P, Sansavini G. Impact of policies on residential multi-energy systems for consumers and prosumers. Appl Energy 2023;344:121276. https://doi.org/10.1016/j.apenergy.2023.121276.

[2] Gutsch M, Leker J. Global warming potential of lithium-ion battery energy storage systems: a review. J Energy Storage 2022;52:105030. https://doi.org/10.1016/j.est.2022.105030.

[3] IEA. Global EV Outlook 2022. IEA; 2022.

[4] Pillot C. The rechargeable battery market and main trends 2020–2030. 2021.

[5] BloombergNEF. Race to Net Zero: The Pressures of the Battery Boom in Five Charts. <https://about.bnef.com/blog/race-to-net-zero-the-pressures-of-the-battery-boom-in-five-charts/>. 2022.

[6] Herrington R. Mining our green future. Nat Rev Mater 2021;6:456–8. https://doi.org/10.1038/s41578-021-00325-9.

[7] Sovacool BK, Ali SH, Bazilian M, Radley B, Nemery B, Okatz J, et al. Sustainable minerals and metals for a low-carbon future. Sci. 2020;367:30–3. https://doi.org/10.1126/science.aaz6003.

[8] Harpprecht C, van Oers L, Northey SA, Yang Y, Steubing B. Environmental impacts of key metals' supply and low-carbon technologies are likely to decrease in the future. J Ind Ecol 2021;25:1543–59. https://doi.org/10.1111/jiec.13181.

[9] The Economist. Could the EV boom run out of juice before it really gets going?. 2022.

[10] The Economist. How supply-chain turmoil is remaking the car industry. 2022.

[11] Mauler L, Duffner F, Leker J. Economies of scale in battery cell manufacturing: The impact of material and process innovations. Appl Energy 2021;286. https://doi.org/10.1016/j.apenergy.2021.116499.

[12] Duffner F, Mauler L, Wentker M, Leker J, Winter M. Large-scale automotive battery cell manufacturing: analyzing strategic and operational effects on manufacturing costs. Int J Prod Econ 2021;232:107982. https://doi.org/10.1016/j.ijpe.2020.107982.

[13] The Economist. Gigafactories are recycling old EV batteries into new ones - it is a further step towards circular manufacturing. 2022.

[14] The Economist. Peter Carlsson on how the global battery race should be run. 2023.

[15] Peiseler L, Bauer C, Beuse M, Wood V, Schmidt TS. Toward a European carbon footprint rule for batteries. Sci. 2022;377:1386–8. https://doi.org/10.1126/science.abp9505.

[16] International Organization for Standardization. ISO 14040:2006. International Organization for Standardization; 2006.

[17] Ciez RE, Whitacre JF. Examining different recycling processes for lithium-ion batteries. Nat Sustain 2019;2:148–56. https://doi.org/10.1038/s41893-019-0222-5.

[18] Dunn J, Kendall A, Slattery M. Electric vehicle lithium-ion battery recycled content standards for the US – targets, costs, and environmental impacts. Res Conserv Recycl 2022;185. https://doi.org/10.1016/j.resconrec.2022.106488.

[19] Philippot M, Alvarez G, Ayerbe E, Mierlo JV, Messagie M. Eco-efficiency of a lithium-ion battery for electric vehicles: Influence of manufacturing country and commodity prices on ghg emissions and costs. Batteries 2019;5. https://doi.org/10.3390/batteries5010023.

[20] Bauer C, Burkhardt S, Dasgupta NP, Ellingsen LAW, Gaines LL, Hao H, et al. Charging sustainable batteries. Nat Sustain 2022;5:176–8. https://doi.org/10.1038/s41893-022-00864-1.

[21] Peters JF, Baumann M, Zimmermann B, Braun J, Weil M. The environmental impact of Li-Ion batteries and the role of key parameters – a review. Renew Sustain Energy Rev 2017;67:491–506. https://doi.org/10.1016/j.rser.2016.08.039.

[22] Kirchain Jr RE, Gregory JR, Olivetti EA. Environmental life-cycle assessment. Nat Mater 2017;16:693–7. https://doi.org/10.1038/nmat4923.

[23] Mauler L, Lou X, Duffner F, Leker J. Technological innovation vs. tightening raw material markets: falling battery costs put at risk. Energy Adv 2022;1:136–45. https://doi.org/10.1039/D1YA00052G.

[24] Armand M, Axmann P, Bresser D, Copley M, Edström K, Ekberg C, et al. Lithium-ion batteries – Current state of the art and anticipated developments. J Power Sources 2020;479. https://doi.org/10.1016/j.jpowsour.2020.228708.

[25] Winjobi O, Kelly JC, Dai Q. Life-cycle analysis, by global region, of automotive lithium-ion nickel manganese cobalt batteries of varying nickel content. Sustain Mater Technol 2022;32. https://doi.org/10.1016/j.susmat.2022.e00415.

[26] Chordia M, Nordelöf A, Ellingsen LAW. Environmental life cycle implications of upscaling lithium-ion battery production. Int J Life Cycle Assess 2021. https://doi.org/10.1007/s11367-021-01976-0.

[27] Baars J, Domenech T, Bleischwitz R, Melin HE, Heidrich O. Circular economy strategies for electric vehicle batteries reduce reliance on raw materials. Nat Sustain 2021;4:71–9. https://doi.org/10.1038/s41893-020-00607-0.

[28] Neumann J, Petranikova M, Meeus M, Gamarra JD, Younesi R, Winter M, et al. Recycling of lithium-ion batteries—current state of the art, circular economy, and next generation recycling. Adv Energy Mater 2022;12. https://doi.org/10.1002/aenm.202102917.

[29] Banza Lubaba Nkulu C, Casas L, Haufroid V, De Putter T, Saenen ND, Kayembe-Kitenge T, et al. Sustainability of artisanal mining of cobalt in DR Congo. Nat Sustain 2018;1:495–504. https://doi.org/10.1038/s41893-018-0139-4.

[30] The Economist. The green revolution will stall without Latin America’s lithium. 2023.

[31] Porzio J, Scown CD. Life-cycle assessment considerations for batteries and battery materials. Adv Energy Mater 2021;11:2100771. https://doi.org/10.1002/aenm.202100771.

[32] Kwade A, Haselrieder W, Leithoff R, Modlinger A, Dietrich F, Droeder K. Current status and challenges for automotive battery production technologies. Nat Energy 2018;3:290–300. https://doi.org/10.1038/s41560-018-0130-3.

[33] Schmuch R, Wagner R, Horpel G, Placke T, Winter M. Performance and cost of materials for lithium-based rechargeable automotive batteries. Nat Energy 2018;3:267–78. https://doi.org/10.1038/s41560-018-0107-2.

[34] Mao J, Ye C, Zhang S, Xie F, Zeng R, Davey K, et al. Toward practical lithium-ion battery recycling: adding value, tackling circularity and recycling-oriented design. Energ Environ Sci 2022;15:2732–52. https://doi.org/10.1039/d2ee00162d.

[35] Harper G, Sommerville R, Kendrick E, Driscoll L, Slater P, Stolkin R, et al. Recycling lithium-ion batteries from electric vehicles. Nature 2019;575:75–86. https://doi.org/10.1038/s41586-019-1682-5.

[36] Li J, Fleetwood J, Hawley WB, Kays W. From materials to cell: state-of-the-art and prospective technologies for lithium-ion battery electrode processing. Chem Rev 2022;122:903–56. https://doi.org/10.1021/acs.chemrev.1c00565.

[37] Zhang J, Muldoon VL, Deng S. Accelerated synthesis of Li(Ni0.8Co0.1Mn0.1)O2 cathode materials using flame-assisted spray pyrolysis and additives. J Power Sources 2022;528. https://doi.org/10.1016/j.jpowsour.2022.231244.

[38] Ahmed S, Nelson PA, Gallagher KG, Susarla N, Dees DW. Cost and energy demand of producing nickel manganese cobalt cathode material for lithium ion batteries. J Power Sources 2017;342:733–40. https://doi.org/10.1016/j.jpowsour.2016.12.069.

[39] Zang G, Zhang J, Xu S, Xing Y. Techno-economic analysis of cathode material production using flame-assisted spray pyrolysis. Energy 2021;218:119504. https://doi.org/10.1016/j.energy.2020.119504.

[40] Dai Q, Kelly JC, Gaines L, Wang M. Life cycle analysis of lithium-ion batteries for automotive applications. Batteries 2019;5. https://doi.org/10.3390/batteries5020048.

[41] Lai X, Gu H, Chen Q, Tang X, Zhou Y, Gao F, et al. Investigating greenhouse gas emissions and environmental impacts from the production of lithium-ion batteries in China. J Clean Prod 2022;372. https://doi.org/10.1016/j.jclepro.2022.133756.

[42] Liu Y, Zhang R, Wang J, Wang Y. Current and future lithium-ion battery manufacturing. iScience 2021;24:102332. https://doi.org/10.1016/j.isci.2021.102332.

[43] Wood III DL, Wood M, Li J, Du Z, Ruther RE, Hays KA, et al. Perspectives on the relationship between materials chemistry and roll-to-roll electrode manufacturing for high-energy lithium-ion batteries. Energy Storage Mater 2020;29:254–65. https://doi.org/10.1016/j.ensm.2020.04.036.

[44] Windisch-Kern S, Gerold E, Nigl T, Jandric A, Altendorfer M, Rutrecht B, et al. Recycling chains for lithium-ion batteries: a critical examination of current challenges, opportunities and process dependencies. Waste Manag 2022;138:125–39. https://doi.org/10.1016/j.wasman.2021.11.038.

[45] Duffner F, Kronemeyer N, Tübke J, Leker J, Winter M, Schmuch R. Post-lithium-ion battery cell production and its compatibility with lithium-ion cell production infrastructure. Nat Energy 2021;6:123–34. https://doi.org/10.1038/s41560-020-00748-8.

[46] Yang XG, Liu T, Wang CY. Thermally modulated lithium iron phosphate batteries for mass-market electric vehicles. Nat Energy 2021;6:176–85. https://doi.org/10.1038/s41560-020-00757-7.

[47] Wood DL, Li J, Daniel C. Prospects for reducing the processing cost of lithium ion batteries. J Power Sources 2015;275:234–42. https://doi.org/10.1016/j.jpowsour.2014.11.019.

[48] Kallitsis E. On the energy use of battery Gigafactories. J Clean Prod 2022;364:132573. https://doi.org/10.1016/j.jclepro.2022.132573.

[49] Crenna E, Gauch M, Widmer R, Wäger P, Hischier R. Towards more flexibility and transparency in life cycle inventories for Lithium-ion batteries. Res Conserv Recycl 2021;170:105619. https://doi.org/10.1016/j.resconrec.2021.105619.

[50] Figgener J, Stenzel P, Kairies KP, Linssen J, Haberschusz D, Wessels O, et al. The development of stationary battery storage systems in Germany - status 2020. J Energy Storage 2021;33. https://doi.org/10.1016/j.est.2020.101982.

[51] Choi D, Shamim N, Crawford A, Huang Q, Vartanian CK, Viswanathan VV, et al. Li-ion battery technology for grid application. J Power Sources 2021;511:230419. https://doi.org/10.1016/j.jpowsour.2021.230419.

[52] Peters JF, Weil M. Providing a common base for life cycle assessments of Li-ion batteries. J Clean Prod 2018;171:704–13. https://doi.org/10.1016/j.jclepro.2017.10.016.

[53] Kittner N, Lill F, Kammen DM. Energy storage deployment and innovation for the clean energy transition. Nat Energy 2017;2:17125. https://doi.org/10.1038/nenergy.2017.125.

[54] Sommerville R, Zhu PC, Rajaeifar MA, Heidrich O, Goodship V, Kendrick E. A qualitative assessment of lithium ion battery recycling processes. Resour Conserv Recycl 2021;165:11. https://doi.org/10.1016/j.resconrec.2020.105219.

[55] International Organization for Standardization. ISO 14044:2006. International Organization for Standardization; 2006.

[56] Nordelöf A, Poulikidou S, Chordia M, Bitencourt de Oliveira F, Tivander J, Arvidsson R. Methodological approaches to end-of-life modelling in life cycle assessments of lithium-ion batteries. Batteries 2019;5. https://doi.org/10.3390/batteries5030051.

[57] Mohr M, Peters JF, Baumann M, Weil M. Toward a cell-chemistry specific life cycle assessment of lithium-ion battery recycling processes. J Ind Ecol 2020;24:1310–22. https://doi.org/10.1111/jiec.13021.

[58] Kallitsis E, Korre A, Kelsall GH. Life cycle assessment of recycling options for automotive Li-ion battery packs. J Clean Prod 2022;371. https://doi.org/10.1016/j.jclepro.2022.133636.

[59] Jiang S, Hua H, Zhang L, Liu X, Wu H, Yuan Z. Environmental impacts of hydrometallurgical recycling and reusing for manufacturing of lithium-ion traction batteries in China. Sci Total Environ 2022;811. https://doi.org/10.1016/j.scitotenv.2021.152224.

[60] Lander L, Cleaver T, Rajaeifar MA, Nguyen-Tien V, Elliott RJR, Heidrich O, et al. Financial viability of electric vehicle lithium-ion battery recycling. iScience 2021;24. https://doi.org/10.1016/j.isci.2021.102787.

[61] Thompson D, Hyde C, Hartley JM, Abbott AP, Anderson PA, Harper GDJ. To shred or not to shred: A comparative techno-economic assessment of lithium ion battery hydrometallurgical recycling retaining value and improving circularity in LIB supply chains. Res Conserv Recycl 2021;175. https://doi.org/10.1016/j.resconrec.2021.105741.

[62] Quan J, Zhao S, Song D, Wang T, He W, Li G. Comparative life cycle assessment of LFP and NCM batteries including the secondary use and different recycling technologies. Sci Total Environ 2022;819. https://doi.org/10.1016/j.scitotenv.2022.153105.

[63] Blömeke S, Scheller C, Cerdas F, Thies C, Hachenberger R, Gonter M, et al. Material and energy flow analysis for environmental and economic impact assessment of industrial recycling routes for lithium-ion traction batteries. J Clean Prod 2022;377. https://doi.org/10.1016/j.jclepro.2022.134344.

[64] Sun X, Luo X, Zhang Z, Meng F, Yang J. Life cycle assessment of lithium nickel cobalt manganese oxide (NCM) batteries for electric passenger vehicles. J Clean Prod 2020;273. https://doi.org/10.1016/j.jclepro.2020.123006.

[65] Wentker M, Greenwood M, Leker J. A bottom-up approach to Lithium-ion battery cost modeling with a focus on cathode active materials. Energies 2019;12:504. https://doi.org/10.3390/en12030504.

[66] Greenwood M, Wentker M, Leker J. A bottom-up performance and cost assessment of lithium-ion battery pouch cells utilizing nickel-rich cathode active materials and silicon-graphite composite anodes. J Power Sour Adv 2021;9:100055. https://doi.org/10.1016/j.powera.2021.100055.

[67] Ciez RE, Whitacre JF. Comparison between cylindrical and prismatic lithium-ion cell costs using a process based cost model. J Power Sources 2017;340:273–81. https://doi.org/10.1016/j.jpowsour.2016.11.054.

[68] Orangi S, Strømman AH. A techno-economic model for benchmarking the production cost of lithium-ion battery cells. Batteries 2022;8. https://doi.org/10.3390/batteries8080083.

[69] Wernet G, Bauer C, Steubing B, Reinhard J, Moreno-Ruiz E, Weidema B. The ecoinvent database version 3 (part I): overview and methodology. Int J Life Cycle Assess 2016;21:1218–30. https://doi.org/10.1007/s11367-016-1087-8.

[70] Ciroth A. ICT for environment in life cycle applications openLCA — a new open source software for life cycle assessment. Int J Life Cycle Assess 2007;12:209. https://doi.org/10.1065/lca2007.06.337.

[71] GreenDelta GmbH. OpenLCA. <https://www.openlca.org/>. 2022.

[72] European Commission. PEFCR Guidance document - Guidance for the development of Product Environmental Footprint Category Rules (PEFCRs) version 6.3. 2018.

[73] Zampori LPR. Suggestions for updating the Product Environmental Footprint (PEF) method. Publications Office of the European Union; 2019.

[74] Fazio S, Castellani V, Sala S, Schau E, Secchi M, Zampori L. Supporting information to the characterisation factors of recommended EF Life Cycle Impact Assessment methods. Ispra; 2018.

[75] Huijbregts MAJ, Steinmann ZJN, Elshout PMF, Stam G, Verones F, Vieira M, et al. ReCiPe2016: a harmonised life cycle impact assessment method at midpoint and endpoint level. Int J Life Cycle Assess 2017;22:138–47. https://doi.org/10.1007/s11367-016-1246-y.

[76] Crenna E, Secchi M, Benini L, Sala S. Global environmental impacts: data sources and methodological choices for calculating normalization factors for LCA. Int J Life Cycle Assess 2019;24:1851–77. https://doi.org/10.1007/s11367-019-01604-y.

[77] Sala S, Cerutti A, Pant R. Development of a weighting approach for the Environmental Footprint. Luxembourg; 2017.

[78] Sala SCE, Secchi M, Pant R. Global normalisation factors for the Environmental Footprint and Life Cycle Assessment. Publication Office of the European Union; 2017.

[79] Dai Q, Spangenberger JS, Ahmed S, Gaines L, Kelly JC, Wang MQ. EverBatt: A closed-loop battery recycling cost and environmental impacts model. 2019.

[80] U.S. Energy Information Administration. Average price of electricity to ultimate customers by end-use sector. <https://www.eia.gov/electricity/monthly/epm_table_grapher.php?t=epmt_5_6_a>. 2023.

[81] Trading Economics. Natural gas. <https://tradingeconomics.com/commodity/natural-gas>. 2023.

[82] Neef CST, Thielmann A. Recycling of lithium-ion batteries: opportunities and challenges for mechanical and plant engineering. Fraunhofer ISI and VDMA; 2021.

[83] International Energy Agency. Projected costs of generating electricity 2020. Paris; 2020.

[84] Benchmark Mineral Intelligence. (2023).

[85] van Oers L, Guinée JB, Heijungs R. Abiotic resource depletion potentials (ADPs) for elements revisited—updating ultimate reserve estimates and introducing time series for production data. Int J Life Cycle Assess 2020;25:294–308. https://doi.org/10.1007/s11367-019-01683-x.

[86] Hauschild MZ, Goedkoop M, Guinée J, Heijungs R, Huijbregts M, Jolliet O, et al. Identifying best existing practice for characterization modeling in life cycle impact assessment. Int J Life Cycle Assess 2013;18:683–97. https://doi.org/10.1007/s11367-012-0489-5.

[87] Rosenbaum RK, Bachmann TM, Gold LS, Huijbregts MAJ, Jolliet O, Juraske R, et al. USEtox—the UNEP-SETAC toxicity model: recommended characterisation factors for human toxicity and freshwater ecotoxicity in life cycle impact assessment. Int J Life Cycle Assess 2008;13:532–46. https://doi.org/10.1007/s11367-008-0038-4.

[88] Kallitsis E, Korre A, Kelsall G, Kupfersberger M, Nie Z. Environmental life cycle assessment of the production in China of lithium-ion batteries with nickel-cobalt-manganese cathodes utilising novel electrode chemistries. J Clean Prod 2020;254. https://doi.org/10.1016/j.jclepro.2020.120067.

[89] Eurostat. Electricity prices for non-household consumers - bi-annual data. <https://ec.europa.eu/eurostat/databrowser/view/nrg_pc_205/default/table?lang=en>. 2023.

[90] Melin HE, Rajaeifar MA, Ku AY, Kendall A, Harper G, Heidrich O. Global implications of the EU battery regulation. Sci. 2021;373:384–7. https://doi.org/10.1126/science.abh1416.

[91] Kelly JC, Wang M, Dai Q, Winjobi O. Energy, greenhouse gas, and water life cycle analysis of lithium carbonate and lithium hydroxide monohydrate from brine and ore resources and their use in lithium ion battery cathodes and lithium ion batteries. Res Conserv Recycl 2021;174:105762. https://doi.org/10.1016/j.resconrec.2021.105762.

[92] Chordia M, Wickerts S, Nordelöf A, Arvidsson R. Life cycle environmental impacts of current and future battery-grade lithium supply from brine and spodumene. Res Conserv Recycl 2022;187. https://doi.org/10.1016/j.resconrec.2022.106634.

[93] Schenker V, Oberschelp C, Pfister S. Regionalized life cycle assessment of present and future lithium production for Li-ion batteries. Res Conserv Recycl 2022;187. https://doi.org/10.1016/j.resconrec.2022.106611.